Original Research

KF4 Anti-Chymotrypsin-like Elastase 1 Antibody and Purified Alpha-1 Antitrypsin Have Similar but Not Additive Efficacy in Preventing Emphysema in Murine Alpha-1 Antitrypsin Deficiency

Andrew J. Devine, BS[1]* Noah J. Smith, BS[2]* Rashika Joshi, MD[3] Brandon Brooks-Patton[4] Jenna Dunham, BS[4] Ansley N. Varisco[5] Emily M. Goodman, MD[6] Qiang Fan, PhD[3] Basilia Zingarelli, MD, PhD[3] Brian M. Varisco, MD[1,2,6,7]

[1]Heritage College of Osteopathic Medicine, Ohio University, Athens, Ohio, United States

[2]College of Medicine, University of Cincinnati, Cincinnati, Ohio, United States

[3]Critical Care Medicine, Cincinnati Children's Hospital Medical Center, Cincinnati, Ohio, United States

[4]Northern Kentucky University, Highland Heights, Kentucky, United States

[5]University of Arkansas at Little Rock, Little Rock, Arkansas, United States

[6]University of Arkansas for Medical Sciences, Little Rock, Arkansas, United States

[7]Arkansas Children's Research Institute, Little Rock, Arkansas, United States

**Authors contributed equally*

Address correspondence to:
Brian M. Varisco, MD
Arkansas Children's Research Institute
13 Children's Way
Little Rock, Arkansas, USA 72202
Phone: (501) 364-7512
Email: bvarisco@uams.edu

Running Head: **KF4 Anti-CELA1 Antibody in AAT-Deficient Emphysema**

Keywords: protease; anti-protease; elastase; emphysema; COPD; alpha-1 antitrypsin

Abbreviations: AAT=Alpha-1 Antitrypsin; CELA1=Chymotrypsin-like Elastase 1; COPD=Chronic Obstructive Pulmonary Disease; MLI=Mean Linear Intercept; PPE=Porcine Pancreatic Elastase

Funding Support:

Varisco	NIH/NHLBI	R01HL141229
Varisco	A1 Foundation	498262
Zingarelli	NIH/NIGMS	R01GM115973

Published online November 26, 2024 https://doi.org/10.15326/jcopdf.2024.0535

Date of Acceptance: November 11, 2024 | ***Publication Online Date***: November 26, 2024

Citation: Devine AJ, Smith NJ, Joshi R, et al. KF4 anti-chymotrypsin-like elastase 1 antibody and purified alpha-1 antitrypsin have similar but not additive efficacy in preventing emphysema in murine alpha-1 antitrypsin deficiency. *Chronic Obstr Pulm Dis.* 2024; Published online November 26, 2024.
https://doi.org/10.15326/jcopdf.2024.0535

This article has an online supplement.

Published online November 26, 2024 https://doi.org/10.15326/jcopdf.2024.0535

Abstract

Alpha-1 antitrypsin (AAT) deficiency is the most common genetic cause of emphysema. Chymotrypsin-like Elastase 1 (CELA1) is a serine protease neutralized by AAT and is important in emphysema progression. *Cela1*-deficiency is protective in a murine models of AAT-deficient emphysema. KF4 anti-CELA1 antibody prevented emphysema in porcine pancreatic elastase (PPE) and cigarette smoke models in wild type mice. We evaluated potential toxicities of KF4 and its ability to prevent emphysema in AAT deficiency. We found Cela1 protein expression in mouse lung, pancreas, small intestine, spleen, and bone marrow. In toxicity studies, mice treated with KF4 25 mg/kg weekly for four weeks showed an elevation in blood urea nitrogen and slower weight gain compared to lower doses or equivalent dose IgG. By histologic grading of tissue injury of the lung, kidney, liver, and heart, there was some evidence of liver injury with KF4 25 mg/kg, but in all tissues, injury was less than in control mice subjected to cecal ligation and puncture. In efficacy studies, KF4 doses as low as 0.5 mg/kg reduced the lung elastase activity of $AAT^{-/-}$ mice treated with 0.2 units of PPE. In this injury model, $AAT^{-/-}$ mice treated with KF4 1 mg/kg weekly, human purified AAT 60 mg/kg weekly, and combined KF4 and AAT treatment had less emphysema than mice treated with IgG 1 mg/kg weekly. However, the efficacy of KF4, AAT, or KF4 & AAT was similar. While KF4 might be an alternative to AAT replacement, combined KF4 and AAT replacement does not confer additional benefit.

Published online November 26, 2024 https://doi.org/10.15326/jcopdf.2024.0535

Introduction

Alpha-1 antitrypsin (AAT) deficiency is the most common genetic factor predisposing people to emphysema (1). Patients typically present in the fourth or fifth decade of life, and despite meta-analyses suggesting only marginal benefit (2), replacement therapy with purified, human AAT is standard of care (3).

AAT is an anti-protease that neutralizes Neutrophil Elastase, Cathepsin G, and Proteinase-3 (4, 5). Our group has shown that AAT also neutralizes and an alveolar type 2 cell-secreted serine protease called Chymotrypsin-like Elastase 1 (CELA1) (6–8). CELA1 plays a physiologic role in the postnatal lung by reducing lung elastase (6) and at baseline *Cela1*$^{-/-}$ mice have slightly smaller alveoli than wild type mice. In antisense oligonucleotide (6) and genetic (7) models of AAT-deficiency, *Cela1*$^{-/-}$ AAT-deficient mice are protected from emphysema. CELA1-AAT protein complexes can be found in human lung indicating that AAT likely neutralized CELA1 by covalent binding (8).

The KF4 anti-CELA1 monoclonal antibody is a mouse IgG1 that covalently binds to a N-terminal region of the CELA1 molecule (8). KF4 protects wild type mice from cigarette-smoke induced emphysema and from emphysema progression following tracheal administration of porcine pancreatic elastase (PPE). Based upon the premise that AAT neutralization of CELA1 plays a key role in the pathogenesis of emphysema in AAT-deficiency, we sought to test whether Cela1-neutralization using KF4 antibody could protect AAT-deficient mice from emphysema and compare its efficacy with AAT replacement therapy. To do so we used previously reported mice that carry deletions of the *Serpina1a*, *Serpina1b*, *Serpina1c*, *Serpina1d*, and *Serpina1e* genes (9).

Published online November 26, 2024 https://doi.org/10.15326/jcopdf.2024.0535

Methods

Animal Use

Animal use was approved by the Cincinnati Children's Hospital Institutional Review board under authorization 2020-0054 (BMV). In addition, we utilized previously collected images from mice utilized under authorization IACUC2021-0087 (BZ). Results from these studies were previously published (10, 11).

Tracheal PPE Administration

Eight to ten week-old male and female C57BL/6J*Serpina1*^{em3Chmu} mice (Called *AAT*$^{-/-}$ hereafter) were anesthetized with 2% isoflurane and suspended by the incisors on a mouse intubating board. The tongue was withdrawn using forceps, and 0.2 units of porcine pancreatic elastase (PPE, Sigma Aldrich, E1250), in 100 µL of PBS was instilled into the oropharyngeal cavity. The nose was occluded with a finger and the mouse remained suspended until began recovering and aspirated the solution. The mouse was recovered in a cage and observed until ambulation resumed. The day of PPE administration was considered day 1.

Lung Tissue Elastase Assay

Lung elastase activity of *AAT*$^{-/-}$ mice treated with different doses of intraperitoneal KF4 was quantified using N-Succinyl-Ala-Ala-Ala-pNitroanilide, substrate for Human Leucocyte Elastase and Porcine Pancreas Elastase (Elastin Products Company #NS945). Lung tissue was homogenized in PBS and 10 mg incubated in the assay for four hours per manufacturer instructions with KF4 or IgG antibody. Signal at 4 hours was used as a measure of elastase activity.

Published online November 26, 2024 https://doi.org/10.15326/jcopdf.2024.0535

KF4 and AAT Treatment

Based on inhibition of lung elastase activity, KF4 1 mg/kg (10 mice), purified human recombinant Alpha-1 Antitrypsin 60 mg/kg (6 mice), combined KF4 and AAT (11 mice), or IgG 1 mg/kg (12 mice) was administered intraperitoneally every seven days starting on day 1 (i.e. the same day as PPE administration) to $AAT^{-/-}$ mice with equal or nearly-equal numbers of male and female mice in each group.

Mouse Cecal Ligation and Puncture

As described previously (10) mice were anesthetized with isoflurane and the cecum visualized through a midline incision The cecum was ligated with 3-0 silk and a single through-and-through puncture made with a 22 gauge needle. Cecal contents were expressed and the abdomen was closed with prolene suture. For sham surgeries, the intestines were manipulated without ligation or puncture. The mice were treated with buprenorphine and recovered. At 6 and 18 hours, mice were sacrificed and vital organs collected.

Tissue Processing

All tissues were fixed in 4% paraformaldehyde in PBS overnight, brought into 100% ethanol by serial dehydration and paraffinized. For liver specimens, only the left lobe was placed in the cassette for embedding. Only the left kidney was embedded. Whole hearts were embedded but only left ventricles assessed. For lung lobes, the four right lung lobes were arranged in a cassette with random orientation and embedded. Five micron sections of each specimen were mounted on a slide and stained using hematoxylin and eosin.

Published online November 26, 2024 https://doi.org/10.15326/jcopdf.2024.0535

Imaging

Using a Nikon Ti2 microscope, for liver, kidney, and heart tissues, five 10X and five 40X images per slide were obtained. For lung images, five 10X images from each lobe were obtained and a total of five 40X images from each lung lobe were obtained.

Mean Linear Intercept Analysis

Using the methods of Dunnill et al (12), after de-identification, mean linear intercept (MLI) values were determined for each 10X lung photomicrograph by a reviewer (AD).

Toxicity Assessment

Procedure: Eight week-old wild type female C57BL6 mice were administered 5, 12.5, or 25 mg/kg KF4 or 25 mg/kg mouse anti-Human IgG (Jackson Laboratories, 711-005-152) peritoneally. For 5, 12.5, and 25 mg/kg doses, a maximum of 5 mg/kg was administered at any given time and antibody was administered 1, 3, and 5 times per week respectively. At six weeks, mice were anesthetized, exsanguinated, and major organs collected for processing as above.

Tissue Injury Scoring

Three blinded scorers (JD, BBP, and ANV) were instructed on how to perform injury scoring of photomicrographs of lung, liver, kidney, and heart tissue using the rubrics in the Online Data Supplement. Tissues from KF4 or IgG treated wild type mice were duplicated and de-identified and a score for each image determined. Unpublished cecal ligation and puncture images were used as positive controls. The average image scores were analyzed by treatment and reviewer agreement assessed.

Published online November 26, 2024 https://doi.org/10.15326/jcopdf.2024.0535

Immunohistochemistry

For immunohistochemistry the ABC Vectastain kit was used with a previously validated anti-CELA1 guinea pig polyclonal antibody (5). Images were obtained using a Nikon TiE microscope.

Immunofluorescence

Mouse bone marrow aspirates and lung sections were immunostained with the same guinea pig antibody and Cd45 (Millipore Cat#05-1410) or pro-Surfactant Protein C (Seven Hills Bioreagents Cat#WRAB-9337) antibodies with appropriate secondary stains.

Statistical Analysis

Ordinal and non-parametric data was analyzed using Kruskal-Wallis test with Dunn's *post hoc* comparison. Parametric mean linear intercept data was compared by one-way ANOVA with Holm-Sidak *post hoc* test. All tests were two-sided and a p-value of less than 0.05 was considered statistically significant. Parametric data is presented as line and whisker plots with lines representing mean and whiskers standard deviation. Non-parametric and ordinal data is presented as box plots.

Interrater reliability measurements are presented as Kirppendorff's alpha values defining excellent agreement as >0.8, good 0.67 to 0.8, moderate 0.5-0.67, and poor <0.5. The R statistical computing platform, rstatix, irr, and ggpubr packages were used for analysis and figure generation (13–16).

Results

Expression of Cela1 in Murine Tissues

Published online November 26, 2024 https://doi.org/10.15326/jcopdf.2024.0535

To understand the potential toxicities of CELA1 inhibition, we first evaluated normalized mRNA counts in the mouse ENCODE transcriptome library using NCBI Gene. Duodenum, small intestine, colon, and spleen samples had the highest count values (Supplemental Figure 1A). Notably, pancreas was not in the list of evaluated tissues. We then performed immunohistochemistry on selected mouse tissues. As expected, expression was strong throughout the pancreas (Figure 1A). In the kidney, a subset of cells that appeared to be distal convoluted tubules had Cela1 protein (Figure 1B). In the small intestine, Cela1 protein was present in enterocytes in the luminal 1/3 of the villus. This staining was intracellular which with that and mRNA expression indicated that this was not from pancreas-secreted Cela1 (Figure 1C). To further identify cell types potentially expressing Cela1 in the spleen and in consideration of our previous finding that there were more numerous leukocytes in the lungs of *Cela1*$^{-/-}$ mice (8), we evaluated what leukocytes were reported has having CELA1 mRNA in the Human Protein Atlas (17). The two cell types with the highest mRNA levels were basophils and Naïve CD4 T-cells (Supplemental Figure 1B). Consistent with *Cela1* expression in Naïve CD4 T-cells, we observed Cela1 staining in the red pulp of the spleen between follicles (Figure 1D) and in CD45-expressing bone marrow cells (Figure 1E). In the mouse lung, Cela1 was expressed in sparse, contained cells (Figure 1F) consistent with its expression in alveolar type 2 cells. These data indicated that Cela1 inhibition could result in digestive, renal, or immunological toxicities.

Toxicity Assessment of KF4 anti-CELA1 Antibody

To test for toxic effects of KF4, we assessed administered intraperitoneal injections totaling 5 mg/kg KF4, 12.5 mg/kg KF4, 25 mg/kg KF4 or 25 mg/kg KF4 weekly for four weeks. We recorded mouse health assessments three times weekly, mouse mass weekly, and at four weeks collected blood for serology and performed blinded tissue injury scoring of mice. Throughout the four weeks, no mouse showed evidence of distress (i.e. scored less than 3 on a 0-3 scale of

Published online November 26, 2024 https://doi.org/10.15326/jcopdf.2024.0535

mouse health). Mice treated with 25 mg/kg KF4 per week had less weight gain than lower dose KF4 or IgG treatment (Figure 2A-B). Serology of these mice after 4 weeks of treatment showed no differences in liver function tests, kidney function tests, myocardial or other muscle injury, or lipid profile except for a slightly higher blood urea nitrogen (BUN) level in KF4 25 mg/kg treated mice (Figure 2C, Supplemental Figure 2). These data suggest mild toxicity in mice treated with KF4 25 mg/kg weekly.

We performed three-reviewer blinded histological scoring of lung, liver, kidney, and heart tissues from these mice. As a positive control, we used tissues from mice subjected to cecal ligation and puncture (CLP)—a mouse sepsis model in which these scoring systems have been validated. Sham treated mice in these experiments were also evaluated. For antibody-treated and control images, three blinded reviewers scored each image on four criteria using the rubrics in the Online Data Supplement.

In histologic evaluation of lung injury, both CLP and sham animals had more evidence of lung injury than antibody-treated animals (Figure 3A). Reviewer 1 consistently scored animals has having a higher level of lung injury resulting in a Krippendorff's alpha coefficient of 0.35, but this difference was similar across groups. In otherwise healthy mice, escalating doses of KF4 do not cause any greater degree of lung injury than that of non-specific immunoglobulin and levels similar to that of an animal undergoing a sham abdominal surgery.

A similar pattern was observed in the liver. The injury levels of both CLP-treated animals had higher injury levels than all other groups, and sham-treated animals had greater injury than KF4 5 mg/kg and 12.5 mg/kg doses. A small but significant increase in liver injury was noted comparing both IgG and KF4 25 mg/kg doses compared to KF4 5 mg/kg (Figure 3B). Inter-reviewer agreement was moderate with a Krippendorff's alpha of 0.54.

Published online November 26, 2024 https://doi.org/10.15326/jcopdf.2024.0535

For kidney analysis, CLP and sham operated animals had higher levels of injury than any of the antibody-treated groups (Figure 3C). There was substantial interrater variability, and agreement was poor with an alpha value of 0.32.

For myocardial injury scoring, only mild injury was noted in the CLP group which was greater than the injury observed in KF4 12.5 mg/kg and IgG 25 mg/kg administration (Figure 3D). Interrater agreement was again poor with an alpha of 0.279.

Taken together these data show evidence of mild liver injury with administration of KF4 or IgG 25 mg/kg that did not result in liver function test abnormalities.

Efficacy of KF4 in Preventing Emphysema

Using the previously described low-dose PPE model of AAT-deficient emphysema (7), we performed a dose titration experiment using lung homogenate from *AAT*$^{-/-}$ mice administered 0.2 units of tracheal PPE and treated with IgG 2 mg/kg, KF4 2 mg/kg or KF4 0.5 mg/kg in a colorimetric elastase activity assay. Both KF4 doses significantly reduced lung elastase activity (Figure 4A). We then performed an efficacy assay by administering the same tracheal PPE dose to *AAT*$^{-/-}$ mice and treating them with IgG 1 mg/kg/week, KF4 1 mg/kg/week, purified human AAT 60 mg/kg/week, or combined KF4 and AAT. These last three treatment groups had less emphysema at 42 days than IgG treatment (Figure 4B). In evaluating tile scanned lung sections, it appeared that this protection was largely due to a reduction in sub-pleural emphysema (Figure 4C-F).

Ability of KF4 to Reduce Human Lung Elastase Activity in AAT-Deficient Emphysema

We obtained archived frozen lung specimens of individuals with mutations in the *SERPINA1* gene and quantified homogenate elastase activity. The set included two, sixteen, six, and one MM, MS, MZ, and ZZ genotype respectively. While there was substantial variability, the elastase activity of MS and MZ specimens was about 40% higher than MM, and ZZ was a little

Published online November 26, 2024 https://doi.org/10.15326/jcopdf.2024.0535

more than double (Figure 5A). Co-incubating specimens (1, 8, 5, and 1 of MM, MS, MZ, and ZZ respectively) with 500 pM, 178 pM, and 70 pM KF4 demonstrated that KF4 reduced elastase activity in all of genotypes although none reached statistical significance (Figure 5B). These data suggest that KF4 can reduce the lung elastase activity of individuals with genetic mutations in the *SERPINA1* gene.

Discussion

In this study, we showed that the KF4 anti-CELA1 antibody and purified human AAT were similarly effective at preventing emphysema in a mouse model of AAT-deficient emphysema and that KF4 has the potential for renal and hepatic toxicity. Combining AAT and KF4 treatment did not result in less emphysema than either treatment alone. These data are supportive of a central role of CELA1 in AAT-deficient emphysema and suggest that selective CELA1 neutralization could be an alternative for purified AAT replacement therapy in AAT-deficient emphysema.

Our murine toxicity studies suggest that KF4 has a therapeutic index of at least 12.5 and that the two toxicities of greatest concern are renal and digestive. Renal toxicity was evidenced by an elevation of blood urea nitrogen, and evidence of histologic liver injury was observed in the highest administered KF4 dose. Although we did not see any elevation of liver injury markers, these may have become elevated with a longer duration experiment. It is likely that reduced mouse weight with KF4 25 mg/kg treatment compared to lower doses and IgG is due intestinal malabsorption. Since IgG is secreted into the intestinal lumen (18), it is likely that both pancreatic and brush border-synthesized Cela1 is neutralized and at 25 mg/kg malabsorption is induced. Stool studies are needed to confirm this. Due to the asynchronous nature of our experiment, we were unable to perform any hematologic assessments which is a limitation of our

Published online November 26, 2024 https://doi.org/10.15326/jcopdf.2024.0535

study. Interestingly, in humans *CELA1* is not expressed in pancreatic acinar cells due to a mutation in *Pancreatic Transcription Factor 1* (19, 20). This coupled with the fact that CELA1 but not CELA2A, CELA2B, CELA3A, or CELA3B is highly conserved in placental mammals (6) and loss of function mutations are more rare in CELA1 than expected (8) suggest an important, non-digestive role for CELA1. In our short-term murine toxicity studies and inhibition studies in emphysema models, at least one of these roles appears to be postnatal lung remodeling with potential intestinal and immune roles that need to be better defined.

We previously reported that *Cela1*$^{-/-}$ mice gain weight at rates comparable to wild type mice (6). The finding of slower weight gain in mice treated with KF4 25 mg/kg compared to IgG 25 mg/kg suggests the possibility that other digestive enzymes are upregulated with Cela1 is absent throughout development; although, we cannot rule out some other developmental effect. The feces of mice treated with KF4 25 mg/kg were indistinguishable from those in other groups, but a biochemical assessment of those feces might reveal important differences.

We chose to employ the low-dose PPE model of AAT-deficient emphysema based on previous work showing that Cela1-ablation protected AAT-deficient mice in this model (7). The model is relatively quick (42 days) and has a high signal to noise ratio, but it does not accurately capture many important clinical elements of AAT-deficient emphysema. *AAT*$^{-/-}$ mice will develop spontaneous emphysema with age which is consistent with the clinical scenario of diagnosing patients with AAT-deficiency after emphysema is discovered in the fourth and fifth decades of life (21). A more rigorous assessment of KF4 in AAT-deficient emphysema needs to test whether it can prevent this age-related emphysema. Another concern with the PPE model is that since KF4 neutralizes one of the proteases that comprises PPE, it may be that the difference between KF4 and IgG is due to modifying the insult rather than intrinsic lung protective effects.

Published online November 26, 2024 https://doi.org/10.15326/jcopdf.2024.0535

Arguing against this is that *Cela1* ablation in *AAT*$^{-/-}$ mice demonstrated similar levels of protection (7), in wild type mice, delaying KF4 initiation by one week also protected mice against PPE-induced emphysema (8).

Our findings are most consistent with our previously described model that CELA1 acts in the progression but not the initiation of emphysema (8). This would explain seemingly contradictory findings that *Cela1*$^{-/-}$ and KF4-treated mice develop less emphysema in response to 6 months of cigarette smoke exposure compared to wild-type or IgG-treated mice, (8) but cigarette smoke-exposed *AAT*$^{-/-}$*&Cela1*$^{-/-}$ mice have slightly but significantly greater emphysema than *AAT*$^{-/-}$ mice (7). Daily cigarette smoke exposure causes persistent inflammation and the activity of leukocyte-associated proteases like neutrophil elastase, cathepsin G, and matrix metalloproteinases are likely greater in this model than in the PPE model used in this study. Since *AAT*$^{-/-}$ mice lack the canonical anti-protease to counter these proteases, they are perhaps more important than Cela1-mediated remodeling in the context of continued inflammation. In wild type mice, endogenous AAT mitigates the activity of these proteases, and the Cela1-effect is more prominent. Exactly how the genetic absence of *Cela1* potentiates the effect of these other proteases, whether and how Cela1 changes the behavior of Naïve CD4 T-cells, and whether these findings also occur with Cela1 inhibition need further study. Such studies are needed because increased inflammation is present in the lungs of AAT-deficient individuals with normal lung function (22), T-cells are activated and bronchus-associated lymphoid tissue larger in AAT-deficiency (23), AAT modulates oxidative activity in neutrophils (24), and AAT seems to play a role in alveolar macrophage function (25).

To the best of our knowledge, this study is the first to use *ex vivo* lung tissue to test whether AAT or any other therapeutic can reduce overall lung elastolytic activity. In the 1970s

Published online November 26, 2024 https://doi.org/10.15326/jcopdf.2024.0535

before electrophoretic shift and molecular diagnosis approaches were available, serum elastase inhibitory capacity was used for diagnosis of Alpha-1 antitrypsin deficiency (26). In a small study, the anti-elastase capacity of alveolar lining fluid was shown to be elevated after treatment with human purified AAT (27). Many studies including the RAPID trial use serum anti-elastase capacity as a measure of efficacy (28). The approach of using lung tissue from genotyped individuals is obviously limited by specimen availability, but it could be a valuable last pre-clinical test of novel compounds and biologics aimed at reducing lung remodeling in AAT-deficiency since there is no intermediate animal model between mice and humans. While our results only neared statistical significance and were limited by a small number of samples, they showed a consistent pattern in which both AAT and KF4 reduced overall lung elastase activity in AAT-deficient lung.

There are several important limitations of this study. First, we did not evaluate long-term toxicity. The fact that all mice gained weight in this study is reassuring, but it may be that with longer exposures, the effects of digestive dysfunction, liver impairment, or renal injury would become more pronounced. AAT-/- mice were not used for toxicity assessment. While toxicities seen in wild type mice could be safely assumed to also affect AAT-/-, it may be that the altered immune or oxidative state of $AAT^{-/-}$ animals would make them more sensitive to toxicities. However, the dose at which injury was observed was 10-fold higher than the therapeutic dose, and it may be that KF4 is effective at even lower doses. KF4 and AAT treatment could have directly impacted the degree of injury as stated above. Lastly, the combination of KF4 and AAT replacement could have caused some amount of injury associated with a higher osmotic load obscuring potential benefit of combination therapy.

Published online November 26, 2024 https://doi.org/10.15326/jcopdf.2024.0535

In conclusion, we found that the KF4 anti-CELA1 antibody and purified human AAT were similarly effective at preventing emphysema in a mouse model of AAT-deficient emphysema but that there was no benefit to combined therapy.

Published online November 26, 2024 https://doi.org/10.15326/jcopdf.2024.0535

Acknowledgements

We would like to thank Mark Brantly at the University of Florida for providing purified, recombinant human alpha-1 antitrypsin.

Author Participation or Contribution Statement

A-Substantial contributions to the conception or design of the work

B-Substantial contribution to the acquisition, analysis, or interpretation of data

C-Drafting the work or revising it critically for important intellectual content

D-Final approval of the version to be published

E-Agreement to be accountable for all aspects of the work in ensuring that questions related to the accuracy or integrity of any part of the work are appropriately investigated and resolved.

Data Sharing Statement: The data used in manuscript presentation is publicly available at 10.6084/m9.figshare.25403464

Declaration of Interest: Brian Varisco and Cincinnati Children's Hospital Medical Center hold patent WO2021108302A1 Cela-1 inhibition for treatment of lung disease.

Published online November 26, 2024 https://doi.org/10.15326/jcopdf.2024.0535

References

1. Busch R, et al. Genetic Association and Risk Scores in a COPD Meta-Analysis of 16,707 Subjects. *American journal of respiratory cell and molecular biology*. [published online ahead of print: February 2017]. https://doi.org/10.1165/rcmb.2016-0331OC.

2. Gotzsche PC, Johansen HK. Intravenous alpha-1 antitrypsin augmentation therapy for treating patients with alpha-1 antitrypsin deficiency and lung disease. *The Cochrane database of systematic reviews*. 2016;9:Cd007851.

3. Adam Wanner MD. Towards New Therapeutic Solutions for Alpha-1 Antitrypsin Deficiency: Role of the Alpha-1 Foundation. *Chronic Obstructive Pulmonary Diseases:Journal of the COPD Foundation*;7(3):147–150.

4. Heinz A, et al. The action of neutrophil serine proteases on elastin and its precursor. *Biochimie*. 2012;94(1):192–202.

5. Guyot N, et al. Unopposed cathepsin G, neutrophil elastase, and proteinase 3 cause severe lung damage and emphysema. *The American journal of pathology*. 2014;184(8):2197–210.

6. Joshi R, et al. Role for Cela1 in Postnatal Lung Remodeling and AAT-deficient Emphysema. *American journal of respiratory cell and molecular biology*. 2018;59(2):167–178.

7. Devine AJ, et al. Chymotrypsin-like Elastase-1 Mediates Progressive Emphysema in Alpha-1 Antitrypsin Deficiency. *Chronic Obstr Pulm Dis*. [published online ahead of print: August 1, 2023]. https://doi.org/10.15326/jcopdf.2023.0416.

Published online November 26, 2024 https://doi.org/10.15326/jcopdf.2024.0535

8. Ojha M, et al. Anti-CELA1 antibody KF4 prevents emphysema by inhibiting stretch-mediated remodeling. *JCI Insight*. 2024;9(1). https://doi.org/10.1172/jci.insight.169189.

9. Borel F, et al. Editing out five Serpina1 paralogs to create a mouse model of genetic emphysema. *Proceedings of the National Academy of Sciences of the United States of America*. [published online ahead of print: February 16, 2018]. https://doi.org/10.1073/pnas.1713689115.

10. Inata Y, et al. Age-dependent cardiac function during experimental sepsis: effect of pharmacological activation of AMP-activated protein kinase by AICAR. *American Journal of Physiology-Heart and Circulatory Physiology*. 2018;315(4):H826–H837.

11. Inata Y, et al. Autophagy and mitochondrial biogenesis impairment contribute to age-dependent liver injury in experimental sepsis: dysregulation of AMP-activated protein kinase pathway. *The FASEB Journal*. 2018;32(2):728–741.

12. Dunnill MS. Quantative Methods in the Study of Pulmonary Pathology. *Thorax*. 1962;17(4):320–328.

13. R Core Team. *R: A Language and Environment for Statistical Computing*. Vienna, Austria: R Foundation for Statistical Computing; 2019.

14. Kassambara A. rstatix: Pipe-Friendly Framework for Basic Statistical Tests. 2020. https://CRAN.R-project.org/package=rstatix. Accessed August 20, 2020.

15. Kassambara A. ggpubr: Publication Ready Plots - Articles - STHDA [Internet]. 2020. http://www.sthda.com/english/articles/24-ggpubr-publication-ready-plots/. Accessed May 15, 2020.

Published online November 26, 2024 https://doi.org/10.15326/jcopdf.2024.0535

16. Gamer M, Lemon J, Fellows I. irr: Various Coefficients of Interrater Reliability and Agreement. 2019. https://CRAN.R-project.org/package=irr.

17. The Human Protein Atlas [Internet]. https://www.proteinatlas.org/. Accessed January 9, 2020.

18. Yoshida M, et al. Human Neonatal Fc Receptor Mediates Transport of IgG into Luminal Secretions for Delivery of Antigens to Mucosal Dendritic Cells. *Immunity*. 2004;20(6):769–783.

19. Rose SD, MacDonald RJ. Evolutionary silencing of the human elastase I gene (ELA1). *Human molecular genetics*. 1997;6(6):897–903.

20. Rose SD, et al. A single element of the elastase I enhancer is sufficient to direct transcription selectively to the pancreas and gut. *Molecular and cellular biology*. 1994;14(3):2048–57.

21. Stockley RA, Parr DG. Antitrypsin deficiency: still more to learn about the lung after 60 years. *ERJ Open Research*. 2024;10(4). https://doi.org/10.1183/23120541.00139-2024.

22. Kokturk N, et al. Lung Inflammation in alpha-1-antitrypsin deficient individuals with normal lung function. *Respiratory Research*. 2023;24(1):1–10.

23. Baraldo S, et al. Immune Activation in α1-Antitrypsin-Deficiency Emphysema. Beyond the Protease–Antiprotease Paradigm. *Am J Respir Crit Care Med*. 2015;191(4):402–409.

24. Hawkins P, et al. In vitro and in vivo modulation of NADPH oxidase activity and reactive oxygen species production in human neutrophils by α1-antitrypsin. *ERJ Open Research*. 2021;7(4). https://doi.org/10.1183/23120541.00234-2021.

Published online November 26, 2024 https://doi.org/10.15326/jcopdf.2024.0535

25. Lee J, et al. Alpha 1 Antitrypsin-Deficient Macrophages Have Impaired Efferocytosis of Apoptotic Neutrophils. *Frontiers in Immunology*. 2020;11. https://doi.org/10.3389/fimmu.2020.574410.

26. Carp H, Janoff A. Possible Mechanisms Of Emphysema in Smokers. *Am Rev Respir Dis*. 1978;118(3):617–621.

27. Wewers MD, et al. Replacement Therapy for Alpha1-Antitrypsin Deficiency Associated with Emphysema. *New England Journal of Medicine*. 1987;316(17):1055–1062.

28. Chapman KR, et al. Intravenous augmentation treatment and lung density in severe α1 antitrypsin deficiency (RAPID): a randomised, double-blind, placebo-controlled trial. *The Lancet*. 2015;386(9991):360–368.

Published online November 26, 2024 https://doi.org/10.15326/jcopdf.2024.0535

Figure 1: Expression of Chymotrypsin-like Elastase 1 in Mouse Tissues. (A) Cela1 was expressed in mouse pancreatic acinar cells. Scale bar = 200 µm. (A') Higher magnification of A. Scale bar = 50 µm. (B) In the adult mouse kidney, Cela1 was present in a subset of tubules that were in a location and with morphology consistent with distal convoluted tubules. Scale bar = 200 µm. (B') Higher magnification of B. Scale bar = 50 µm. (C) Jejunum from the mouse showed staining in cells and/or debris in the lumen and in the luminal quarter of the villus. Scale bar = 1000 µm. (C') Magnifying the distal villus showed intracellular staining of enterocytes. Scale bar = 100 µm (D) In the spleen, Cela1 staining was seen between follicles which is consistent with Naïve CD4 T-cell location. (D') higher magnification of E. Scale bar = 200 µm. (E) Bone marrow cells from an adult mouse were stained for the leukocyte marker Cd45 (green) and Cela1. Some leukocytes contained Cela1 (yellow arrow) while others did not (green arrow). (F) Mouse lung contained an abundance of alveolar type 2 cells marked by pro-Surfactant protein C (pro-Sftpb, green) with the majority not containing Cela1 (green arrow) and some having Cela1 (yellow arrow). Scale bar = 250 µm. Created with BioRender.com.

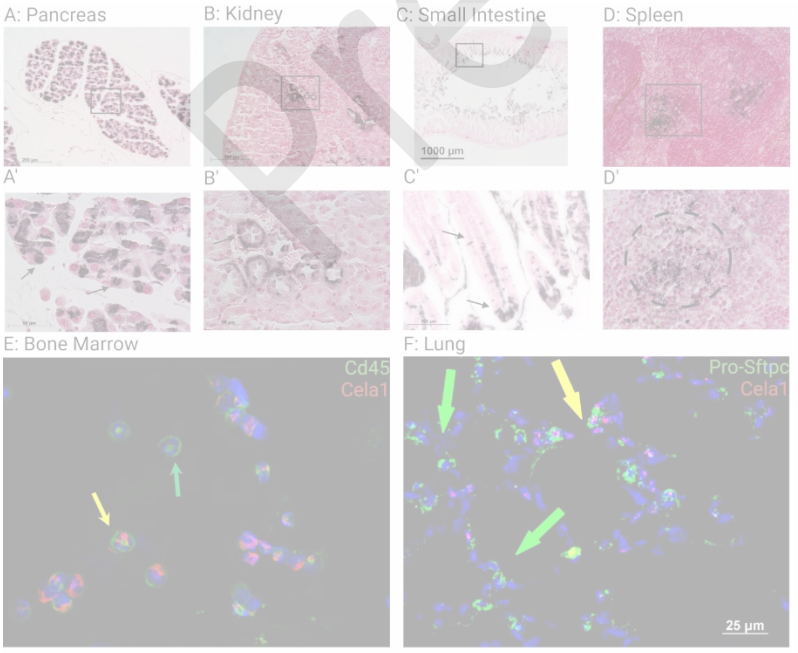

Published online November 26, 2024 https://doi.org/10.15326/jcopdf.2024.0535

Figure 2: Mouse Mass and Serology Toxicity Assessments. (A) Four weeks of treatment with KF4 25 mg/kg resulted in slower weight gain compared with 5 and 12.5 mg/kg KF4 and IgG 25 mg/kg. (B) comparing each treatment group at 7, 14, 21, and 28 days, by one-way ANOVA, days 7 and 21 had a significant difference between groups and in both cases the 25 mg/kg KF4 group had less weight gain than 5 mg/kg KF4 group. * $p<0.05$, ***$p<0.001$ by Holm Sidak *post hoc* test. (B) Blood urea nitrogen (BUN) was significantly higher in KF4 25 mg/kg compared to KF4 12.5 mg/kg treated mice ($p<0.05$). Created with BioRender.com.

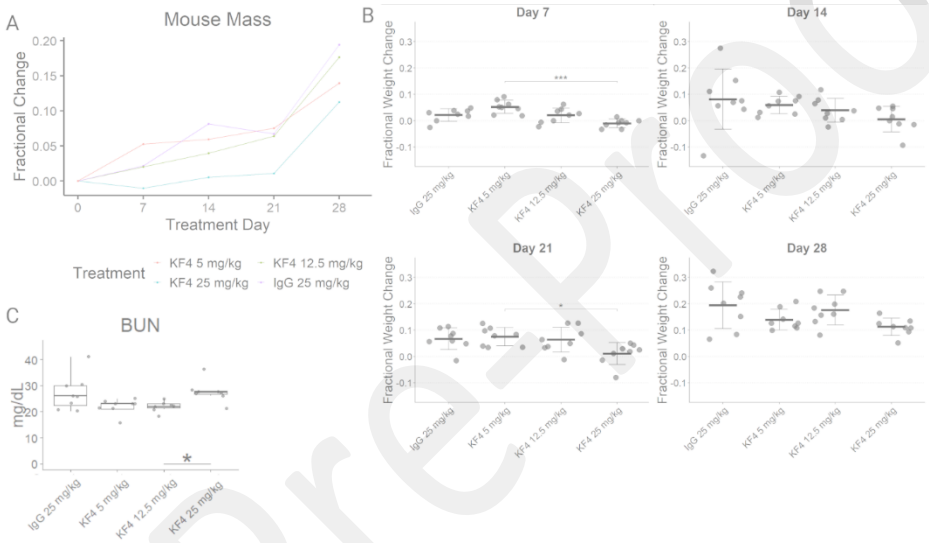

Published online November 26, 2024 https://doi.org/10.15326/jcopdf.2024.0535

Figure 3: Tissue Injury Scoring. (A) Lung injury was less in KF4 and IgG treatment groups compared to lung from animals following cecal ligation and puncture (CLP). (B) Liver injury was also lower in antibody treatment groups but there was increased injury in KF4 25 mg/kg and IgG 25 mg/kg compared to KF4 5 mg/kg. (C) Kidney injury was less with KF4 or IgG treatment compared to sham and CLP animals. (D) Myocardial injury scores were elevated in CLP compared to KF4 12.5 mg/kg and IgG 25 mg/kg treatments, but the absolute difference was small. *p<0.05, **p<0.01, ***p<0.001, ****p<0.00001 by Dunn's post hoc test. Created with BioRender.com.

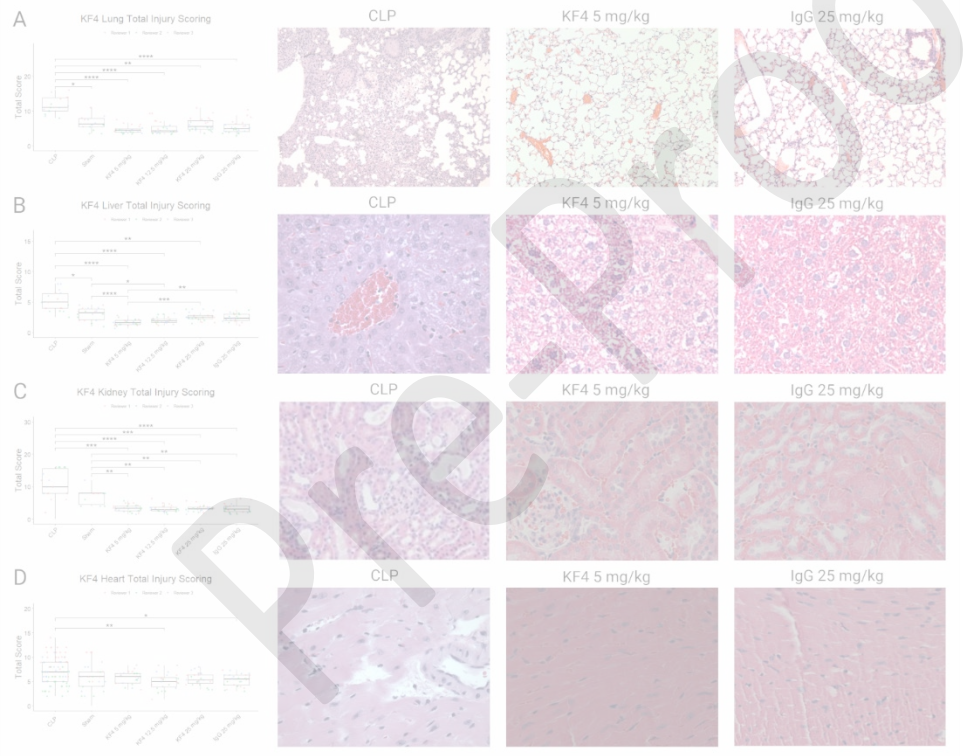

Published online November 26, 2024 https://doi.org/10.15326/jcopdf.2024.0535

Figure 4: KF4 Treatment in AAT-deficient Emphysema Model. (A) At 21 days after 0.2 units of tracheal porcine pancreatic elastase, the lungs of *AAT*$^{-/-}$ mice treated with weekly KF4 0.5 mg/kg and KF4 2 mg/kg had less total elastase activity than those treated with IgG 2 mg/kg. *p<0.05, **p<0.01 by Dunn's post hoc test. (B) Treating *AAT*$^{-/-}$ mice exposed to 0.2 units of tracheal PPE with IgG 1 mg/kg, KF4 1 mg/kg, purified human AAT 60 mg/kg, or combined AAT and KF4 showed less emphysema in the latter three groups compared to the first. *p<0.05, **p<0.01, **** p<0.0001 by Dunn's post hoc test. (C) Tile scanned middle lobe lung section of an IgG-treated mouse showing substantial emphysema. Scale bar = 500 µm. (D) KF4-treatement had less emphysema as did (E) AAT treatment. (F) Combined treatment also had less emphysema, and in each of these there was a lack of sub-pleural airspace simplification. Created with BioRender.com.

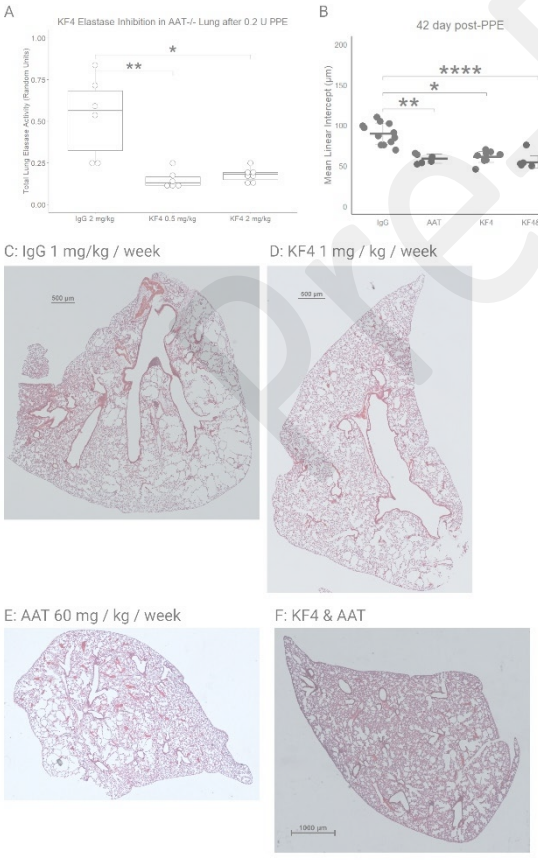

Published online November 26, 2024 https://doi.org/10.15326/jcopdf.2024.0535

Figure 5: Human Lung Elastase Activity with Mutations in *SERPINA1*. (A) Lung homogenates from archived specimens of individual with zero mutations in the SERPINA1 gene (MM, n=2), one mutation (MS n=16 and MZ n=6) or homozygous mutation (ZZ n=1) were assessed for total lung elastase activity. While no statistical comparison could be made because a group contained only one specimen, there was a pattern of increased elastase activity in heterozygotes and yet higher activity in the homozygous mutation. (B) Co-incubating these specimens with KF4 (500, 278, or 70 fM final concentration) showed trends towards reduced lung elastase activity.

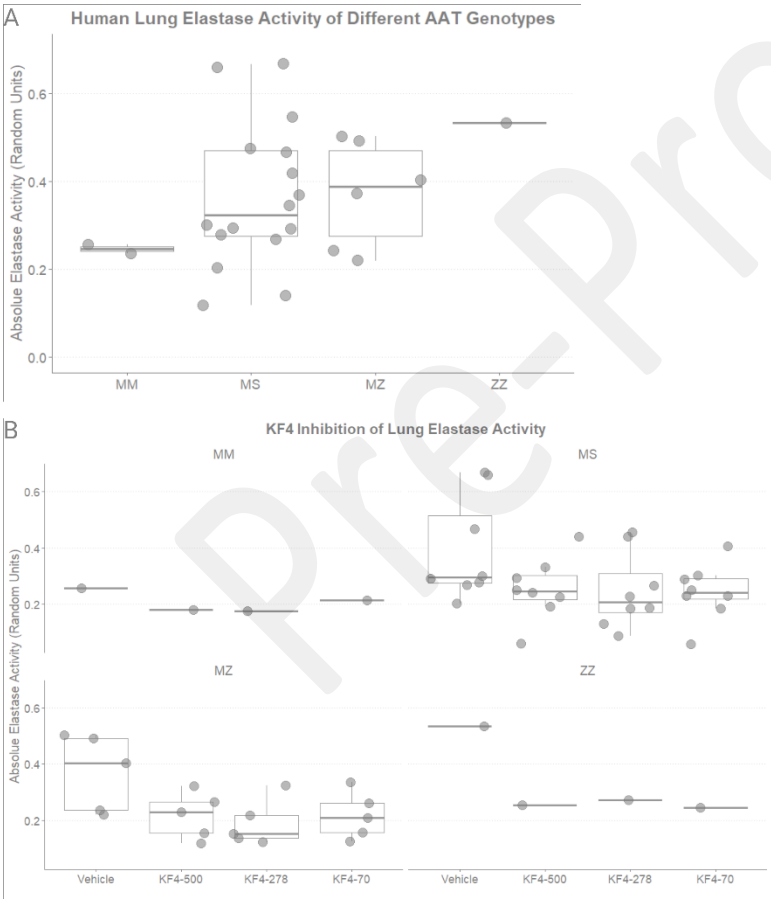

Published online November 26, 2024 https://doi.org/10.15326/jcopdf.2024.0535

Online Supplement

Supplement: KF4 anti-CELA1 Antibody and Purified α1-Antitrypsin Have Similar but Not Additive Efficacy in Preventing Emphysema in Murine α1-Antitrypsin Deficiency

Supplemental Methods

Serology

At the time of animal sacrifice, 1 mL of blood was aspirated using a needle in the vena cava prior to exsanguination and major organ harvest. Plasma was stored at -80°C and sent to IDEXX Bioanalytics for aspartate aminotransferase (AST), alanine aminotransferase (ALT), alkaline phosphatase (ALP), total bilirubin, blood urea nitrogen (BUN), creatinine, phosphorus, creatine kinase, triglyceride, total cholesterol, high density lipoprotein (HDL), glucose, albumin, and total protein quantification.

Supplemental Figures

Supplemental Figure 1: CELA1 Expression in Published Datasets. (A) Assessment of mRNA levels of various mouse tissues showed that the highest Cela1 mRNA levels were in the small intestine, spleen, and kidney. FKPM = Fragments per kilobase per Million mapped reads. (B) To identify what types of cells might be expressing Cela1 in the spleen, we used a query tool in the Human Protein Atlas which indicated highest expression in basophils and Naïve CD4 T-cells. nTPM = normalized transcripts per million.

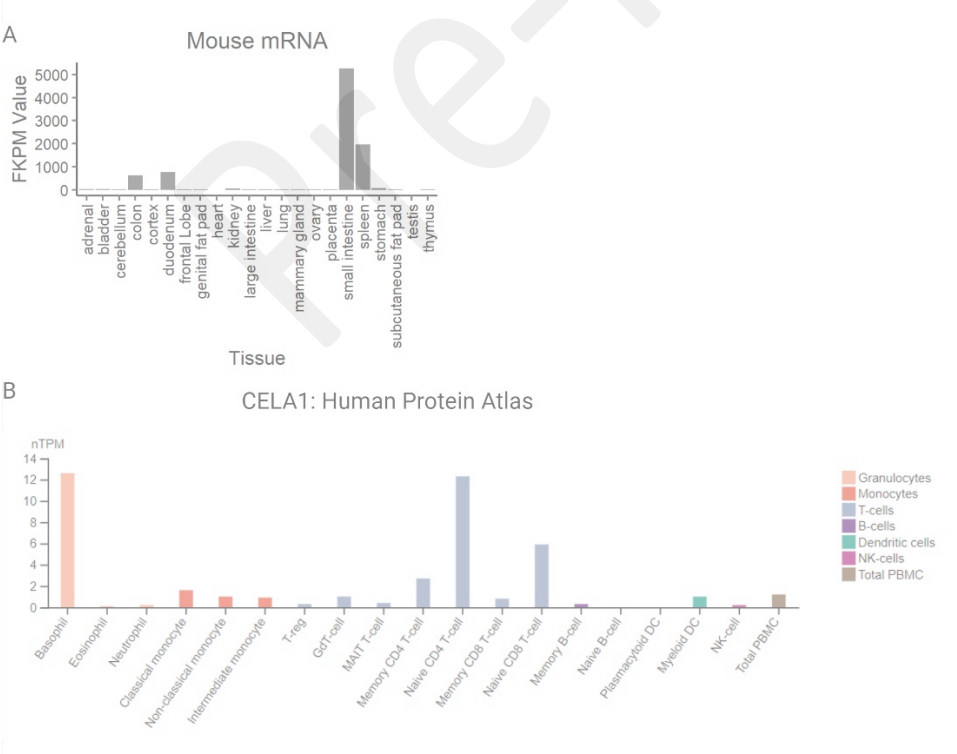

Published online November 26, 2024 https://doi.org/10.15326/jcopdf.2024.0535

Supplemental Figure 2: Serum Toxicity Analysis. Serology from mice identified no differences in aspartate aminotransferase (AST), alanine aminotransferase (ALT), alkaline phosphatase (ALP), total bilirubin, creatinine, phosphorus, creatine kinase, triglyceride, total cholesterol, high density lipoprotein (HDL), glucose, albumin, or total protein.

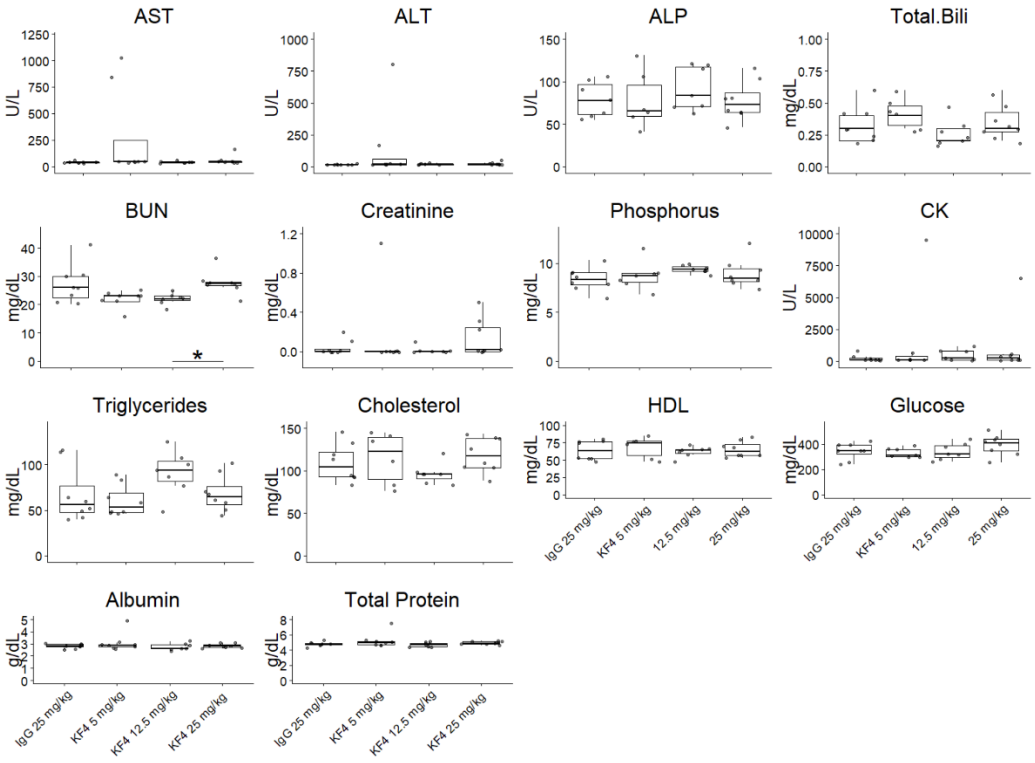

Published online November 26, 2024 https://doi.org/10.15326/jcopdf.2024.0535

Histological signs of lung injury

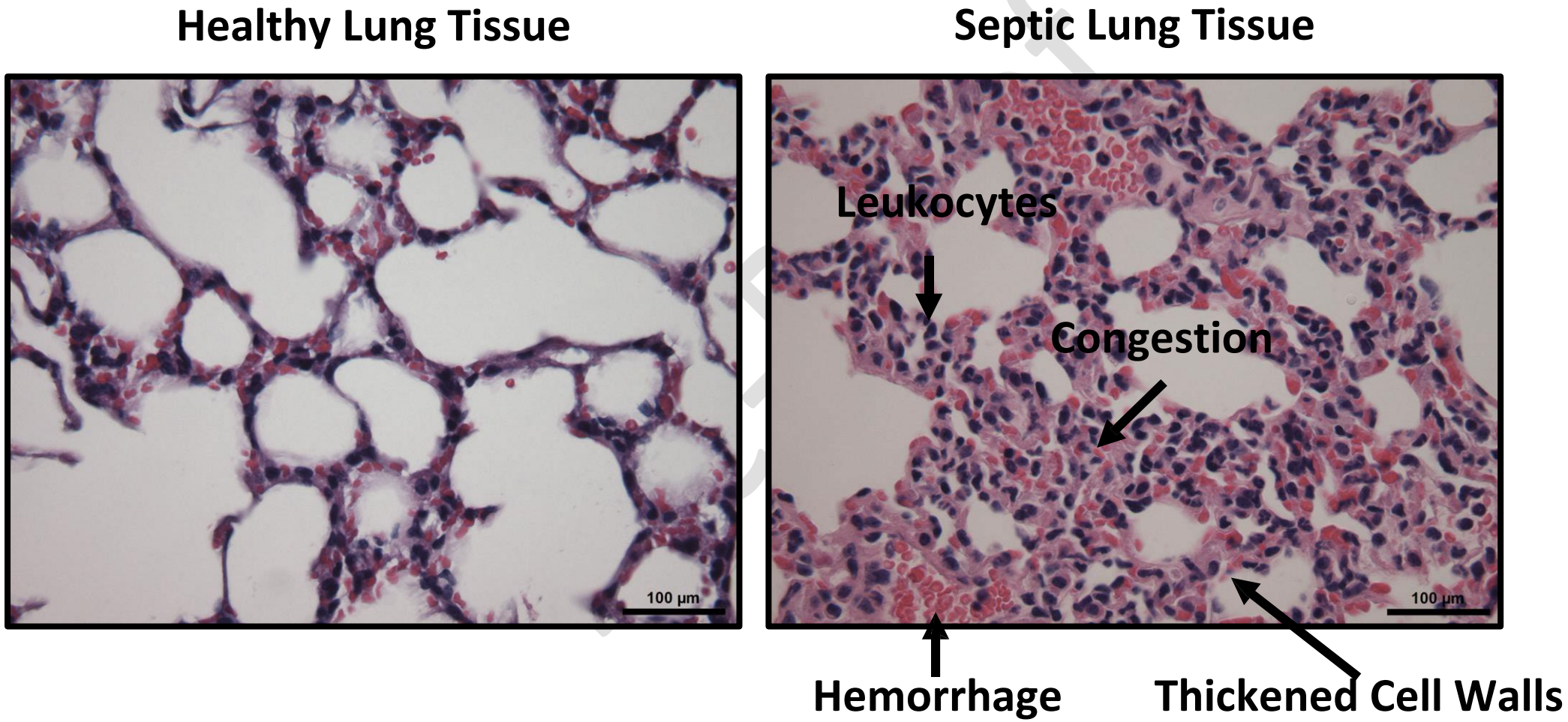

Published online November 26, 2024 https://doi.org/10.15326/jcopdf.2024.0535

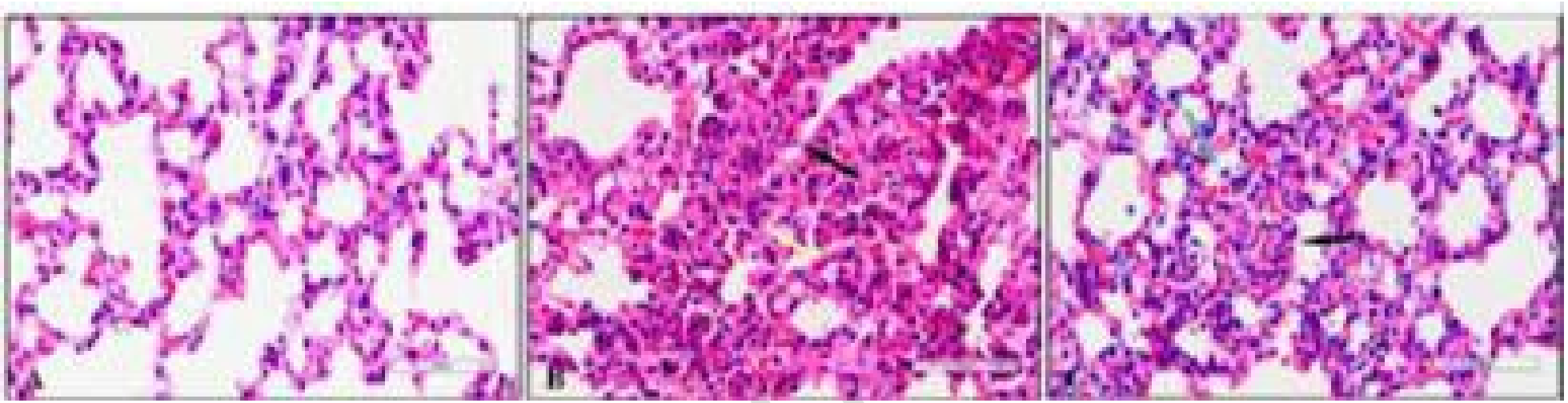

Scores

0 = no injury
1 = minimal (0-25%of the section)
2 = mild (25-50%)
3 = significant (50-75%)
4 = severe (more than 75%)

Published online November 26, 2024 https://doi.org/10.15326/jcopdf.2024.0535

Alveolar Congestion or Reduction of Alveolar Space	1	3	2
Hemorrhage	1	3	3
Infiltration of Leukocytes into Airspace or Alveolar Walls	2	3	3
Thickness of Alveolar Wall or Hyaline Membrane Formation	2	4	3
Total	6	13	11

Published online November 26, 2024 https://doi.org/10.15326/jcopdf.2024.0535

Scores

0 = no injury
1 = minimal (0-25%of the section)
2 = mild (25-50%)
3 = significant (50-75%)
4 = severe (more than 75%)

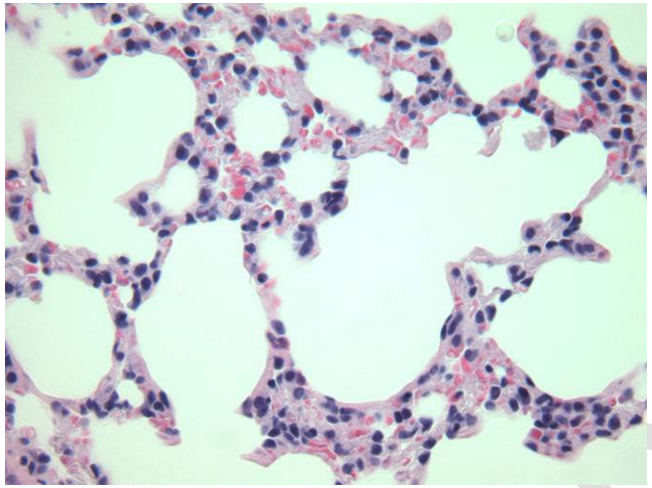

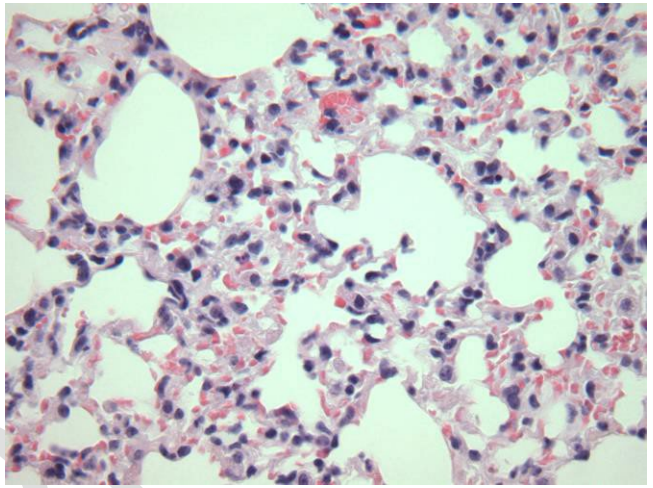

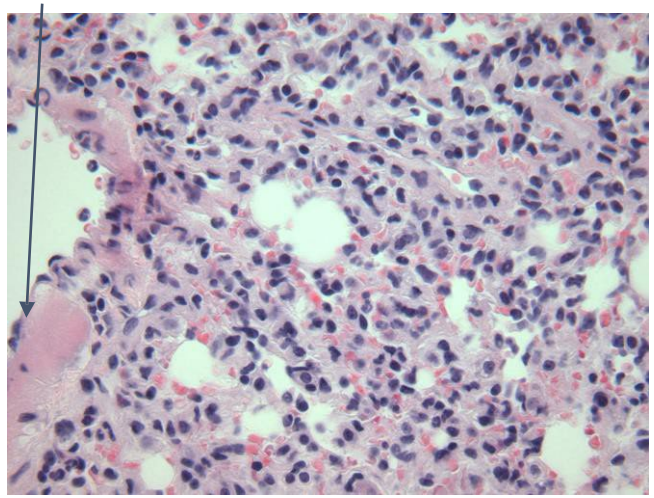

Alveolar Congestion or Reduction of Alveolar Space	1	2	3
Hemorrhage	0	1	1
Infiltration of Leukocytes into Airspace or Alveolar Walls	2	2	3

Published online November 26, 2024 https://doi.org/10.15326/jcopdf.2024.0535

Thickness of Alveolar Wall or Hyaline Membrane Formation	1	2	4
Total	4	7	11

Published online November 26, 2024 https://doi.org/10.15326/jcopdf.2024.0535

Scores

0 = no injury
1 = minimal (0-25%of the section)
2 = mild (25-50%)
3 = significant (50-75%)
4 = severe (more than 75%)

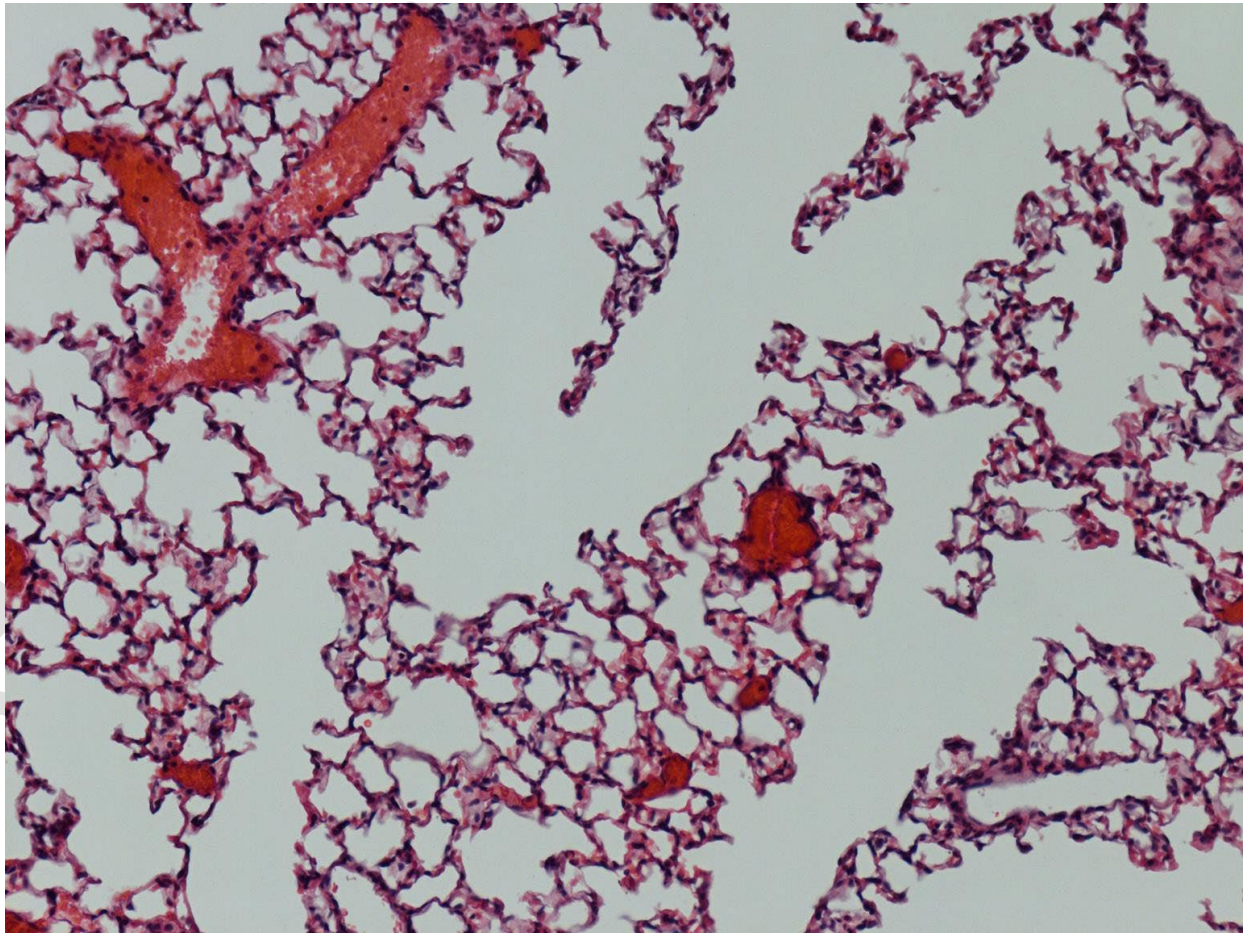

Published online November 26, 2024 https://doi.org/10.15326/jcopdf.2024.0535

Alveolar Congestion or Reduction of Alveolar Space	0
Hemorrhage	0
Infiltration of Leukocytes into Airspace or Alveolar Walls	1
Thickness of Alveolar Wall or Hyaline Membrane Formation	2 (hyaline membranes)
Total	3

Published online November 26, 2024 https://doi.org/10.15326/jcopdf.2024.0535

Histological Signs of Liver Injury

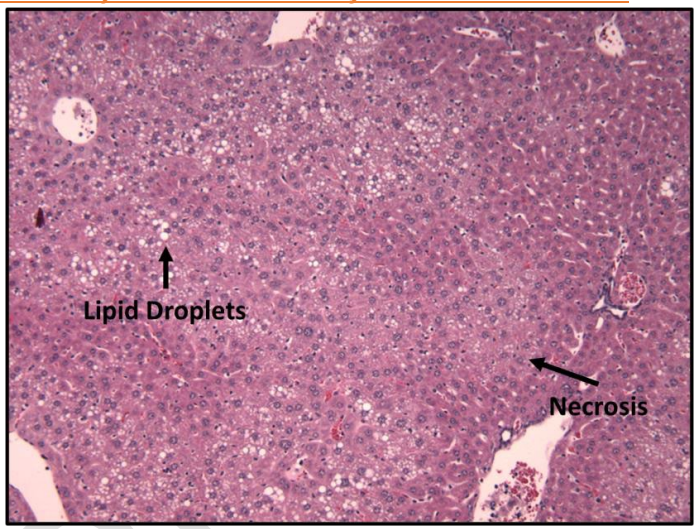

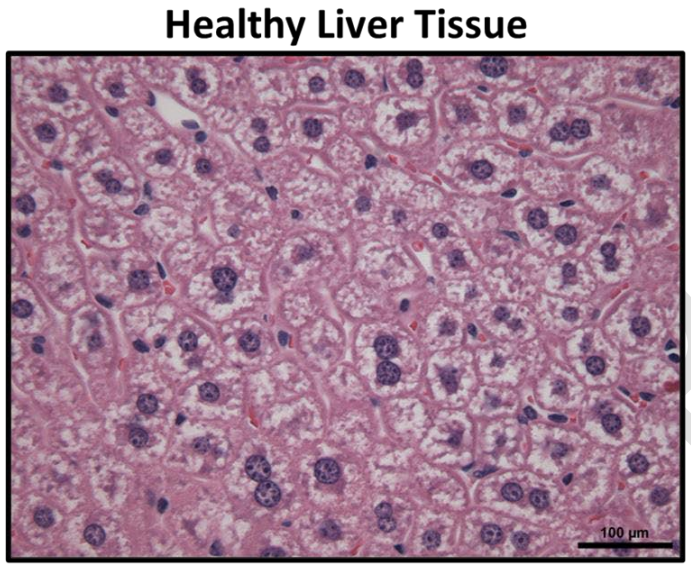

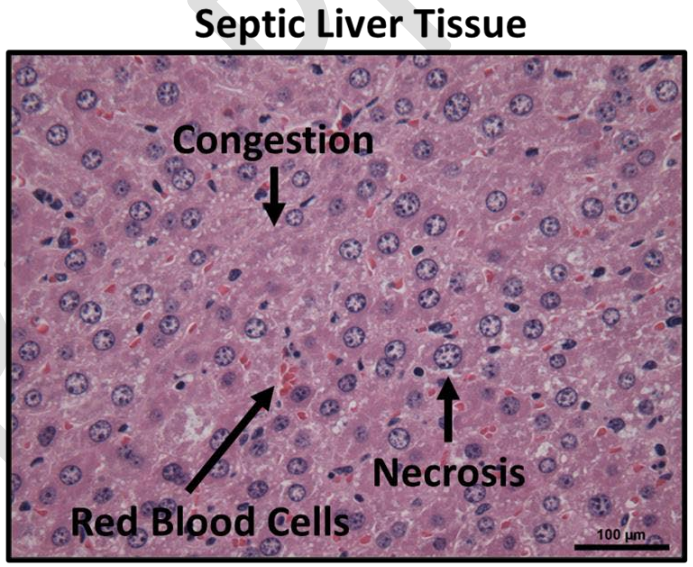

Published online November 26, 2024 https://doi.org/10.15326/jcopdf.2024.0535

Scores

0 = no injury
1 = minimal (0-25%of the section)
2 = mild (25-50%)
3 = significant (50-75%)
4 = severe (more than 75%)

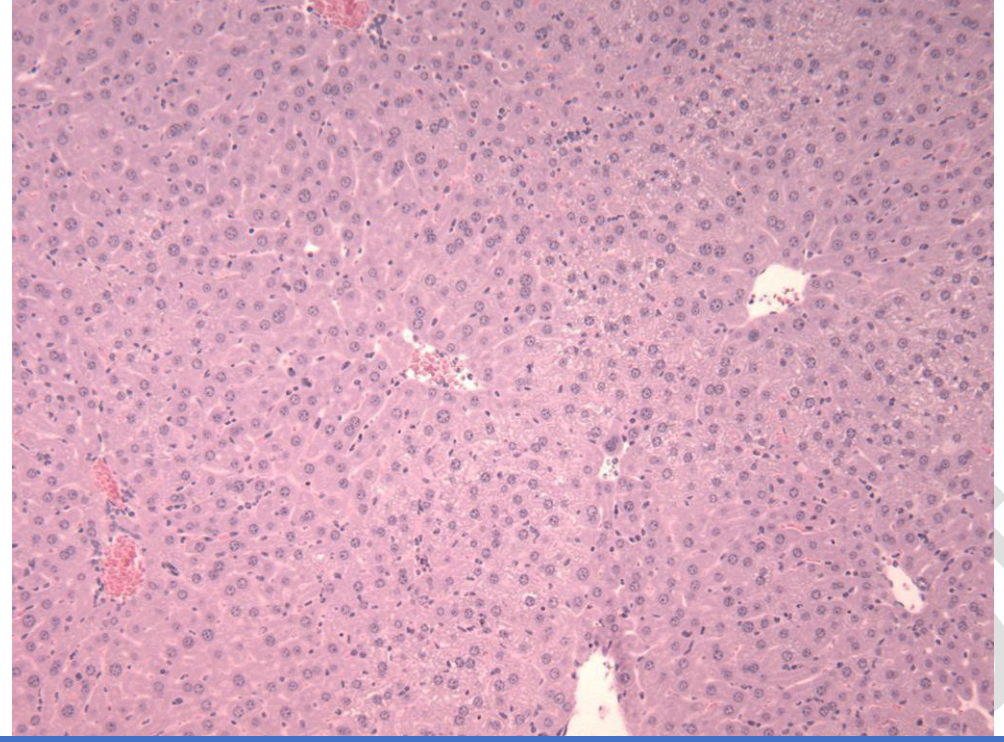

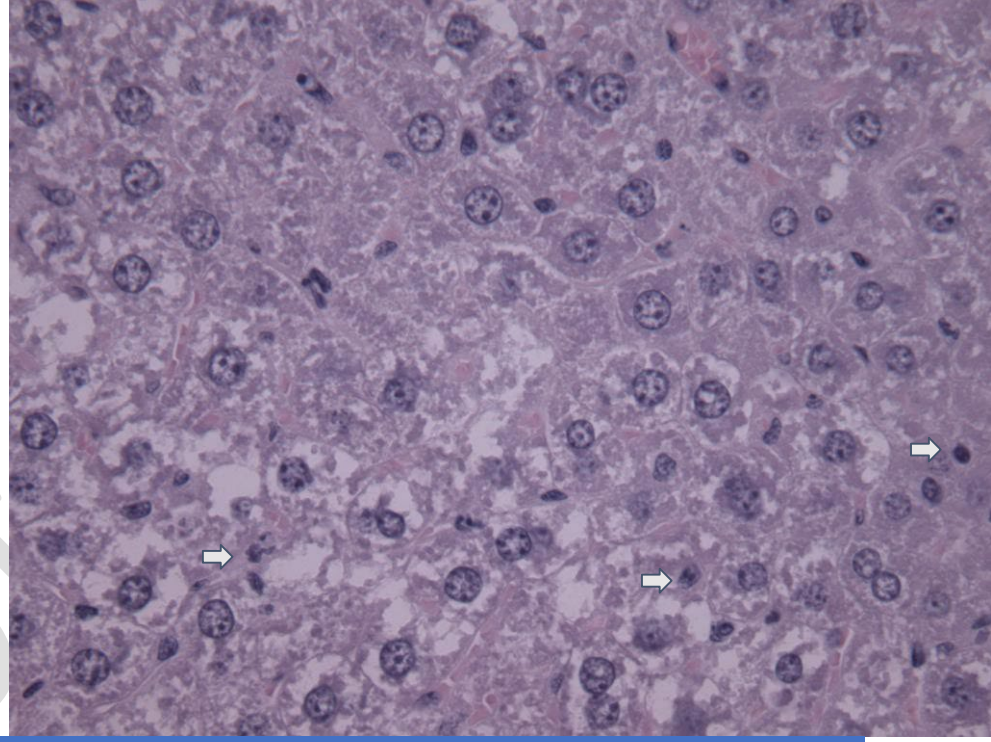

	10x	40x
Sinusoid congestion and/or edema (10X)	3	
Infiltration of red blood and inflammatory cells (10X)	2	
Presence of lipid droplets or vacuoles (10 & 40X)	0	0
Necrosis (10 & 40X)	3	3

Scores

0 = no injury
1 = minimal (0-25%of the section)
2 = mild (25-50%)
3 = significant (50-75%)
4 = severe (more than 75%)

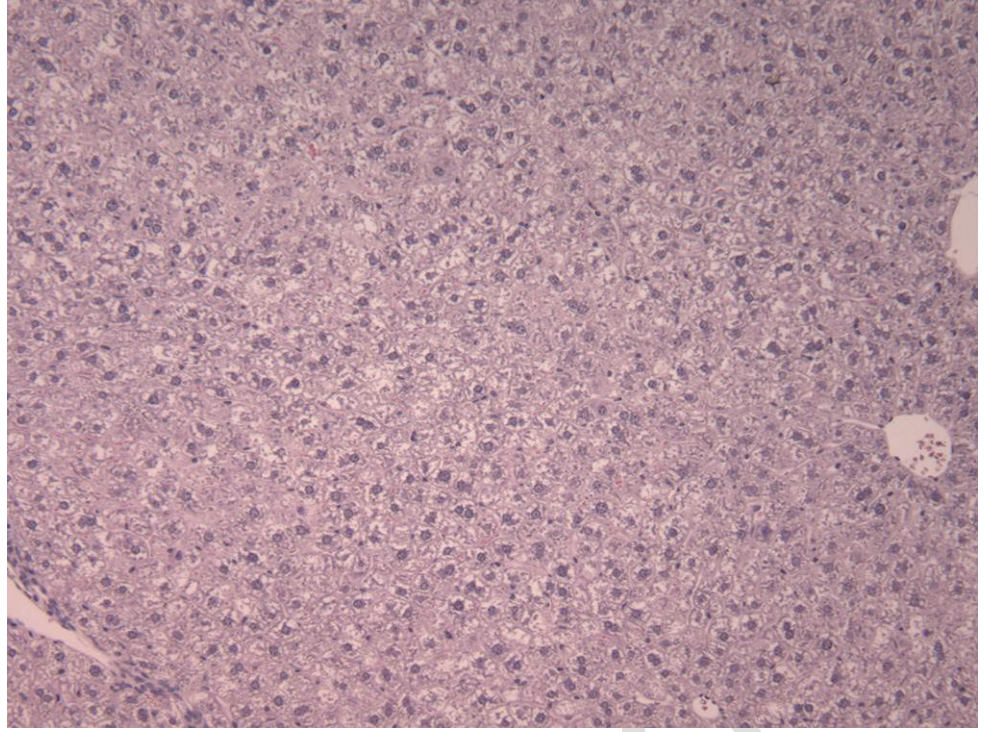

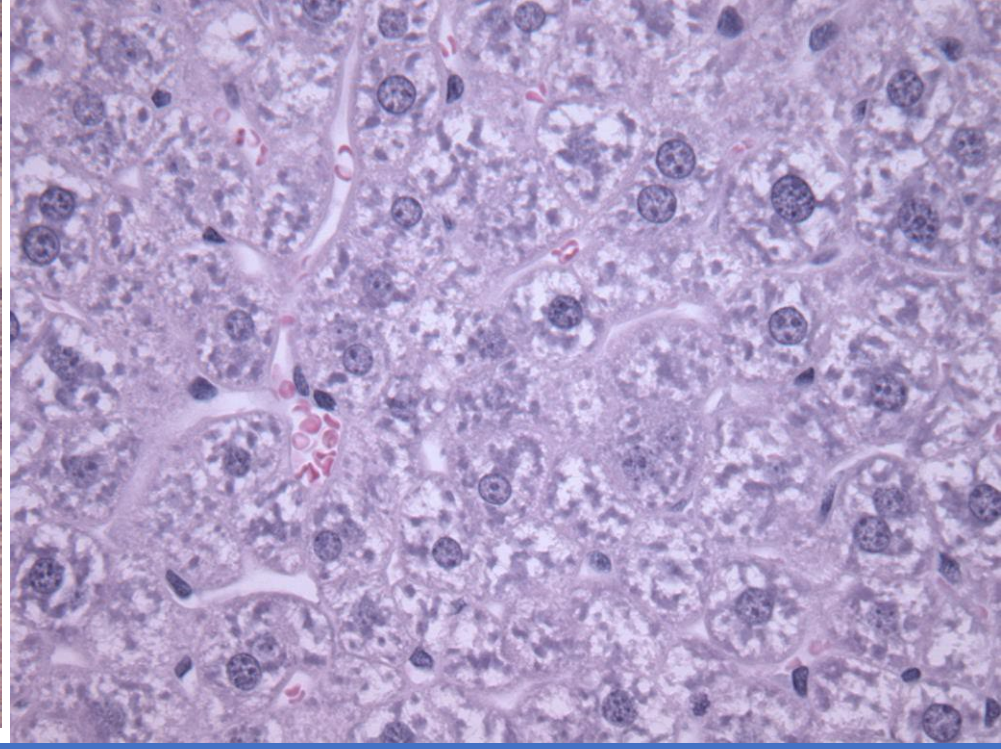

	10x	40x
Sinusoid congestion and/or edema (10X)	0	
Infiltration of red blood and inflammatory cells (10X)	0	
Presence of lipid droplets or vacuoles (10 & 40X)	0	0
Necrosis (10 & 40X)	1	1

Scores

0 = no injury
1 = minimal (0-25%of the section)
2 = mild (25-50%)
3 = significant (50-75%)
4 = severe (more than 75%)

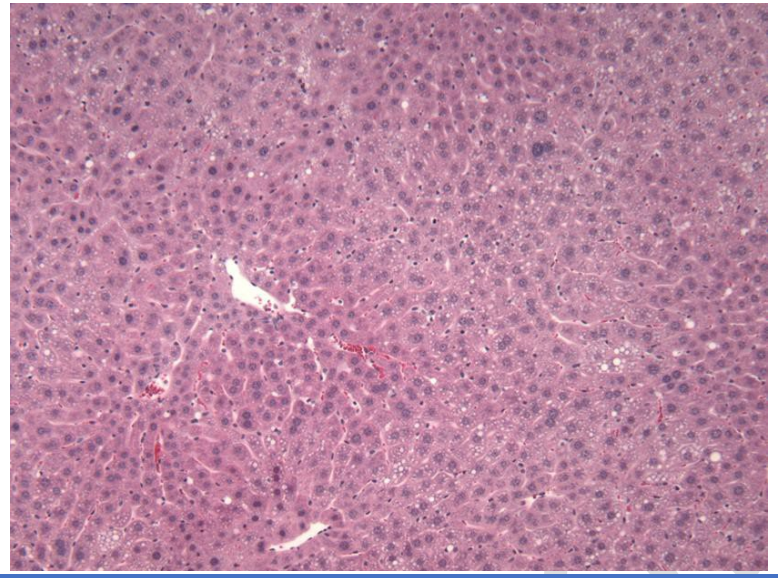

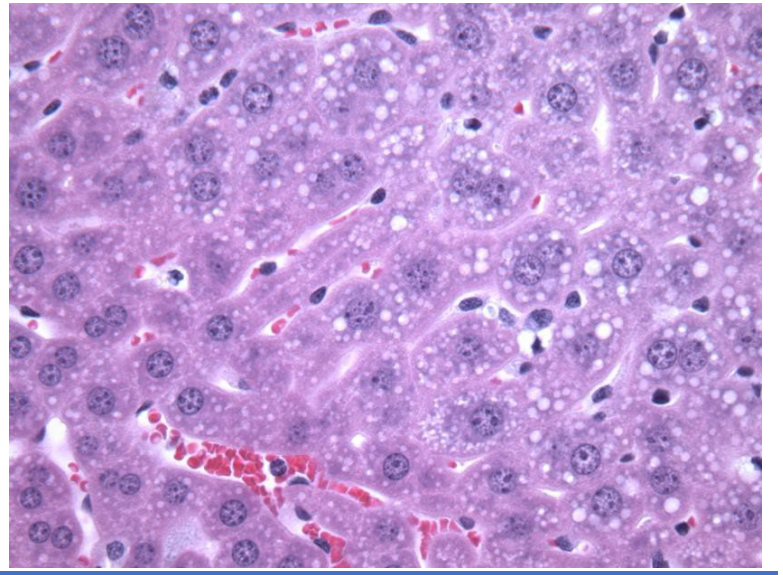

	10x	40x
Sinusoid congestion and/or edema (10X)	3	
Infiltration of red blood and inflammatory cells (10X)	3	
Presence of lipid droplets or vacuoles (10 & 40X)	3	4
Necrosis (10 & 40X)	3	3
Total		

Histological signs of kidney injury-10X

Healthy Kidney Tissue

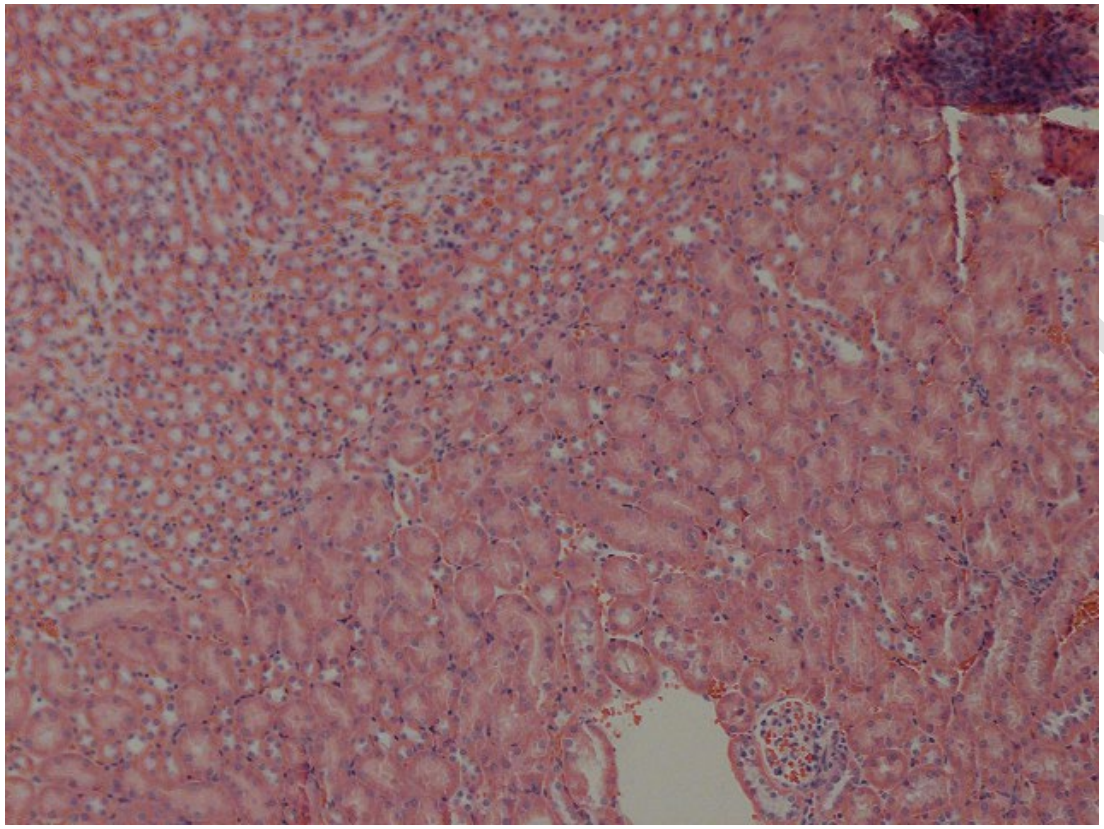

I/R Kidney Tissue

Leukocytes

Hemorrhage

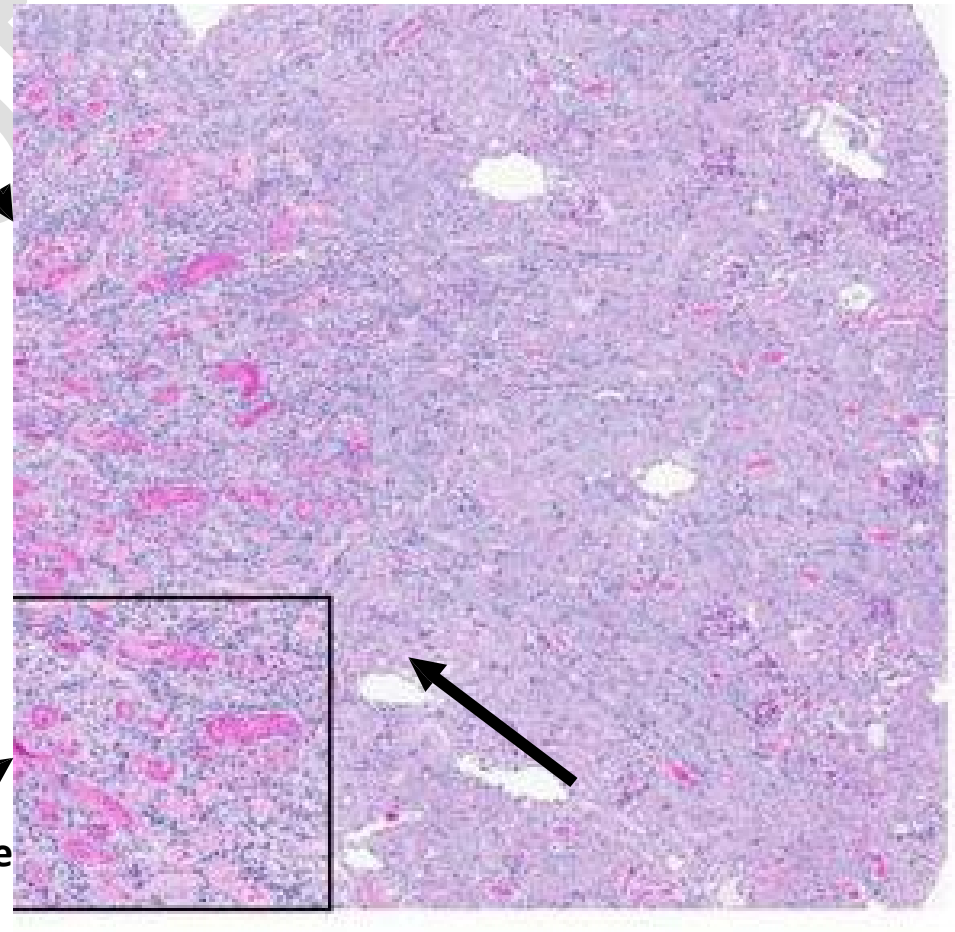

Histological signs of kidney injury-40X

Healthy Kidney Tissue

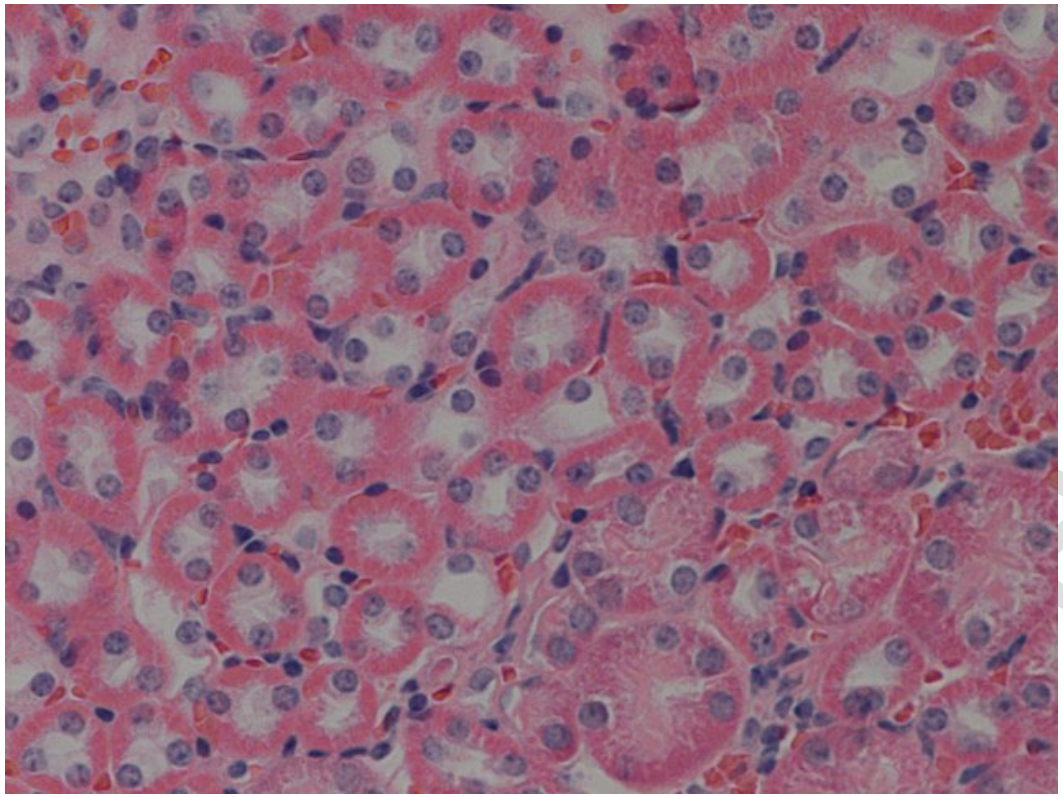

I/R Kidney Tissue

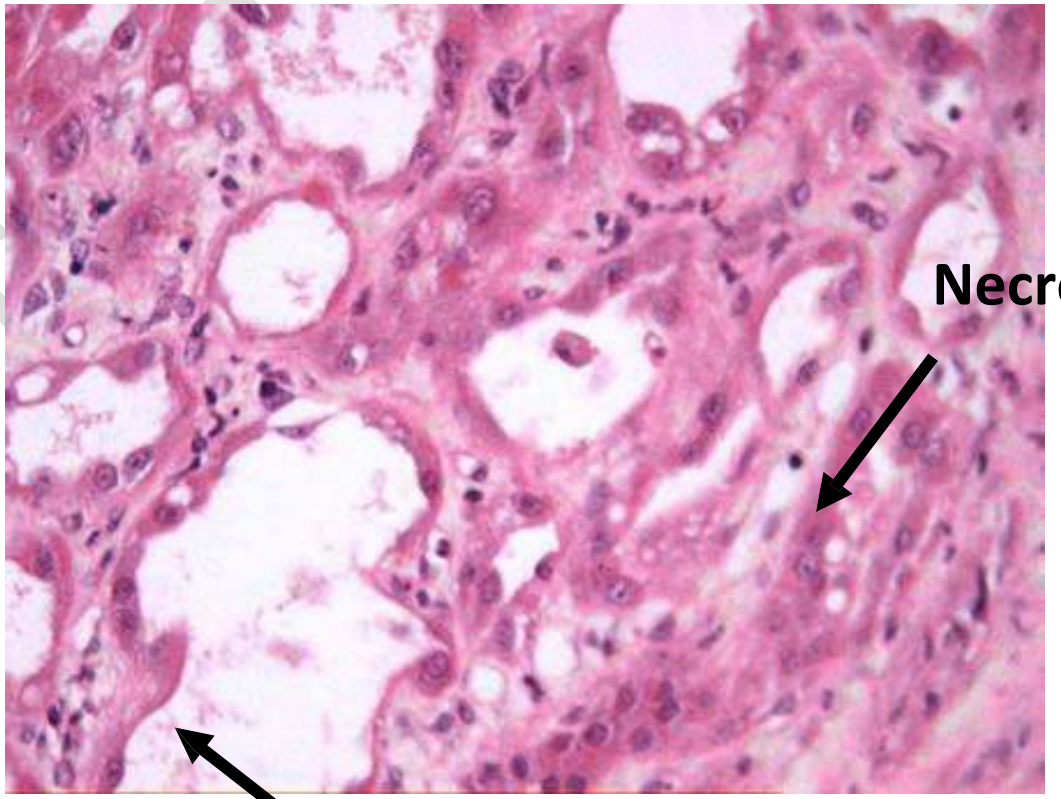

Scores

0 = no injury
1 = minimal (0-25%of the section)
2 = mild (25-50%)
3 = significant (50-75%)
4 = severe (more than 75%)

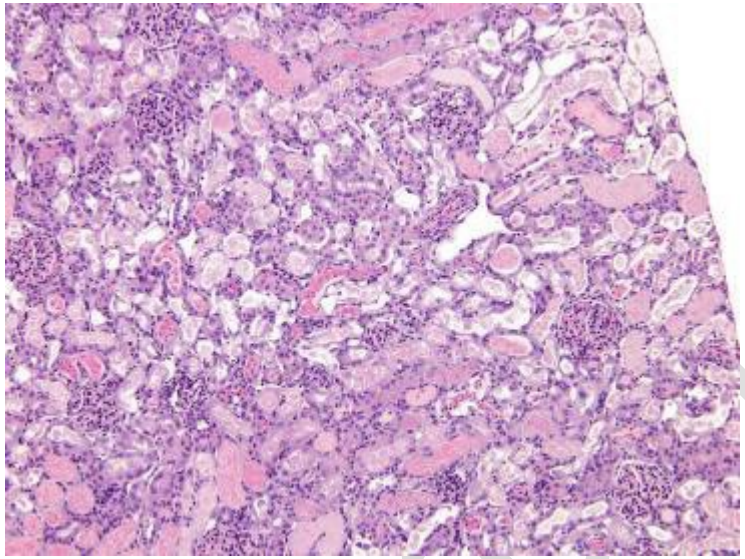

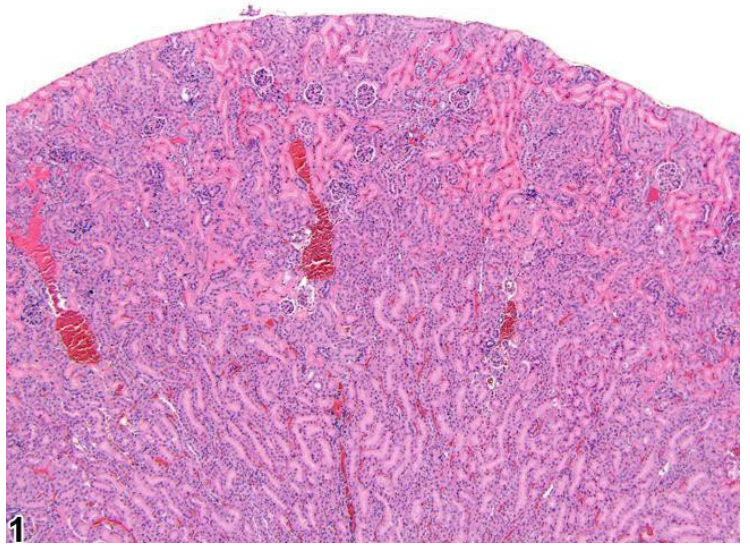

Loss of Brush Border (40X)		
Tubular Necrosis (40X)		
Neutrophil Infiltration (10X)	3	4
Hemorrhage/Congestion (10x)	1	3
Total	4	7

Scores

0 = no injury
1 = minimal (0-25%of the section)
2 = mild (25-50%)
3 = significant (50-75%)
4 = severe (more than 75%)

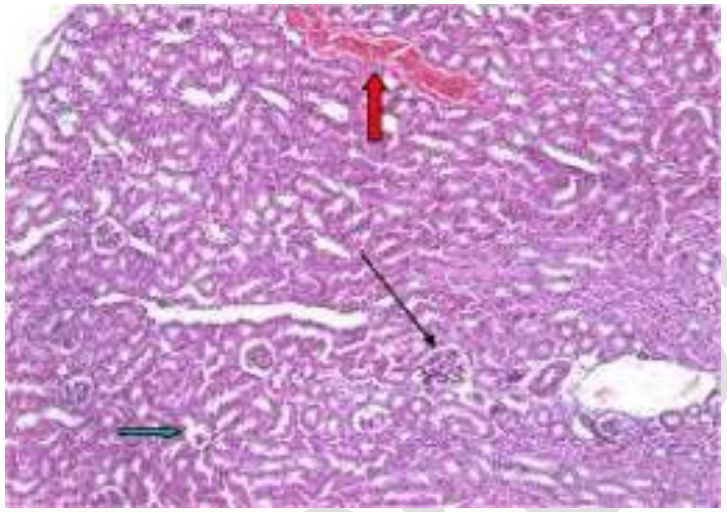

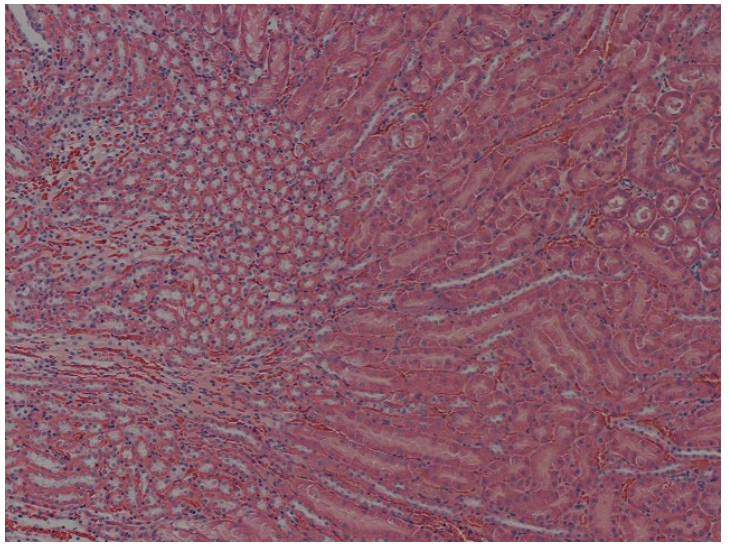

Loss of Brush Border (40X)		
Tubular Necrosis (40X)		
Neutrophil Infiltration (10X)	0	0
Hemorrhage/Congestion (10x)	1	0
Total	1	0

Adrenal Gland

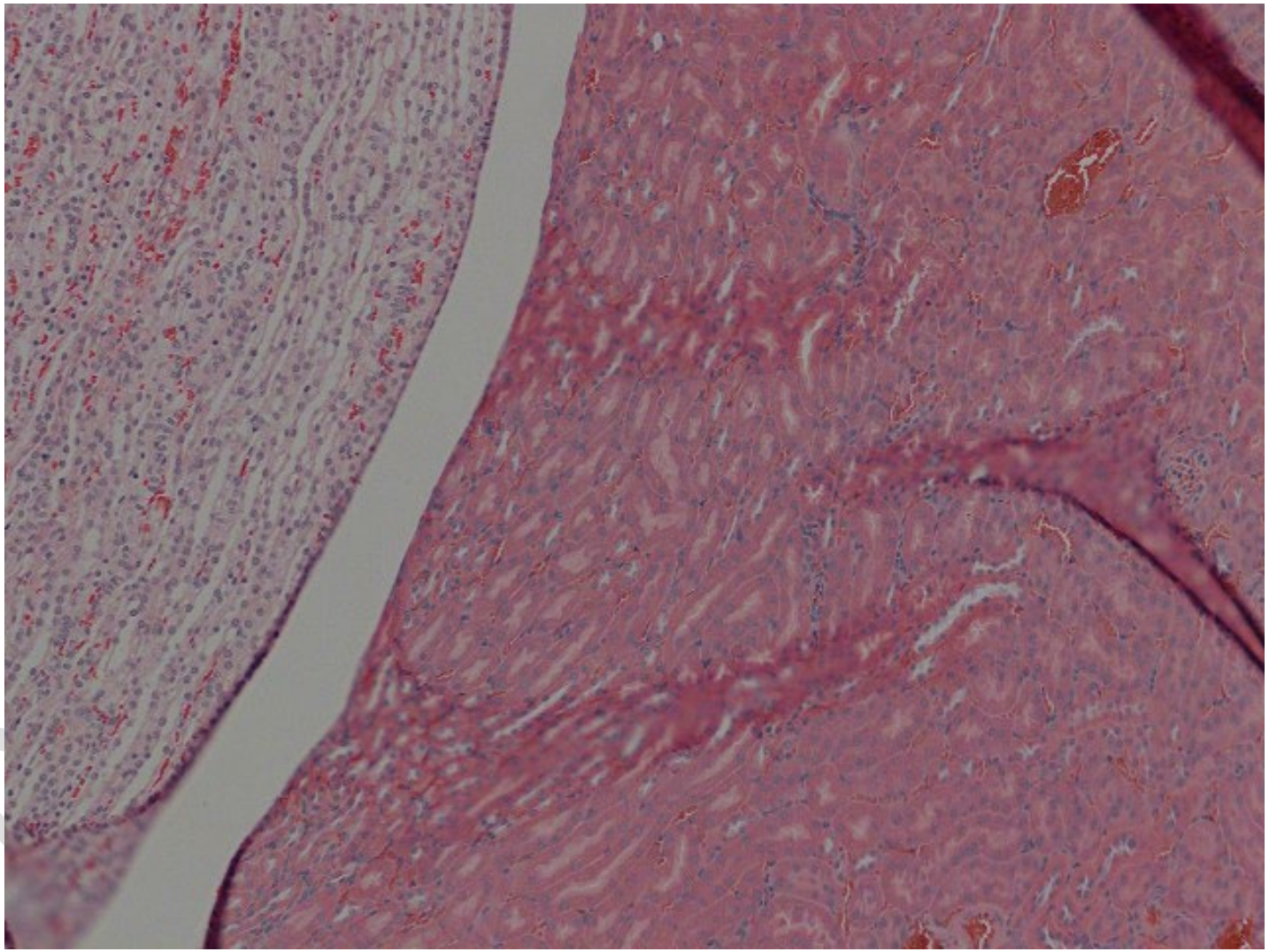

Scores

0 = no injury
1 = minimal (0-25%of the section)
2 = mild (25-50%)
3 = significant (50-75%)
4 = severe (more than 75%)

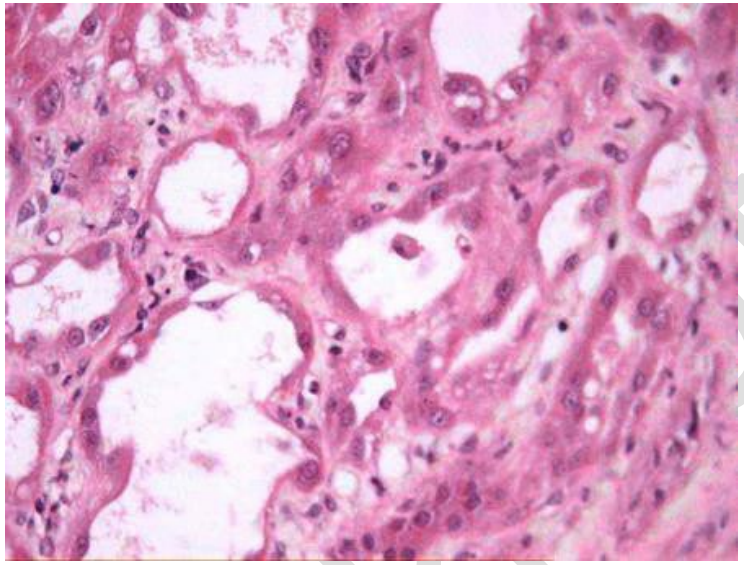

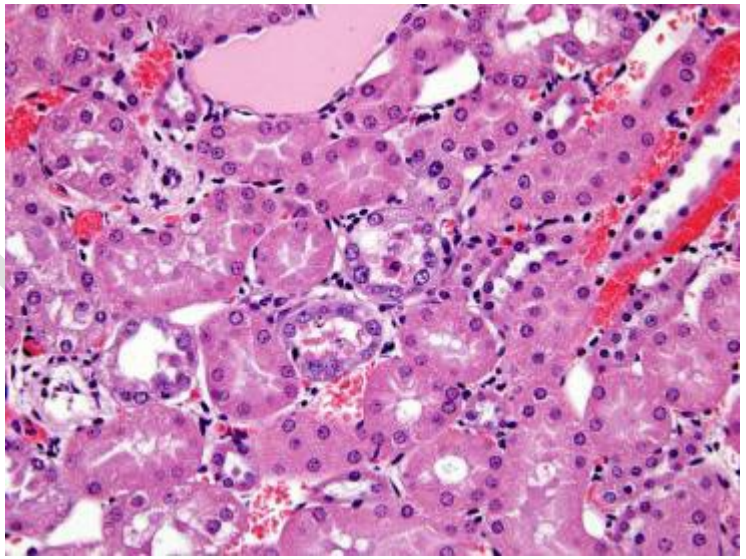

Loss of Brush Border (40X)	4	2
Tubular Necrosis (40X)	4	3
Neutrophil Infiltration (10X)		
Hemorrhage/Congestion (10x)		
Total	8	5

0 = no injury
1 = minimal (0-25%of the section)
2 = mild (25-50%)
3 = significant (50-75%)
4 = severe (more than 75%)

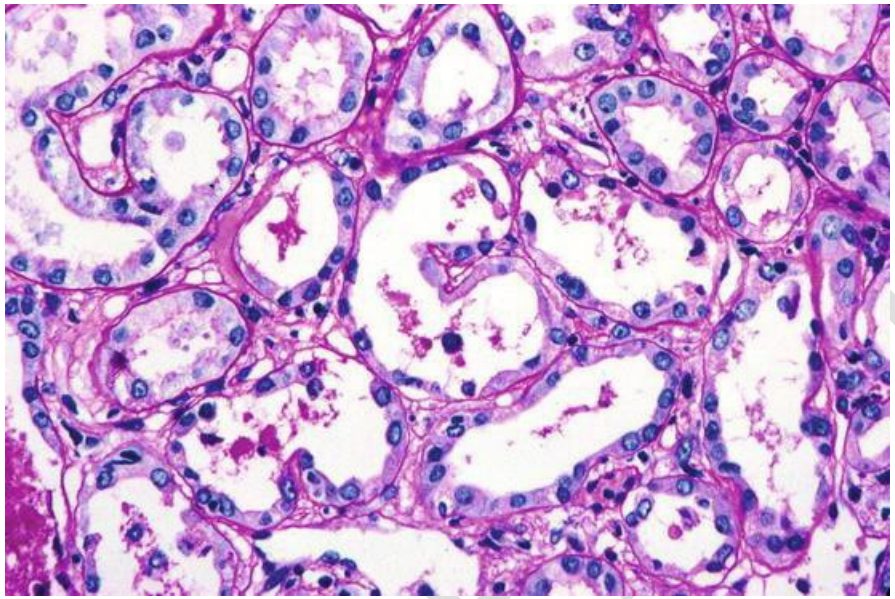

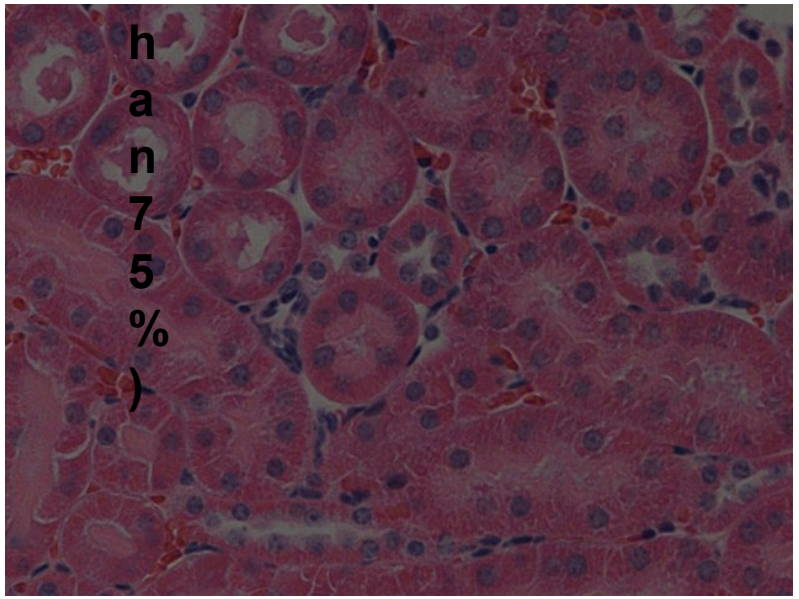

Loss of Brush Border (40X)
Tubular Necrosis (40X)
Neutrophil Infiltration (10X)
Hemorrhage/Congestion (10x)
Total

Histological Signs of Heart Injury

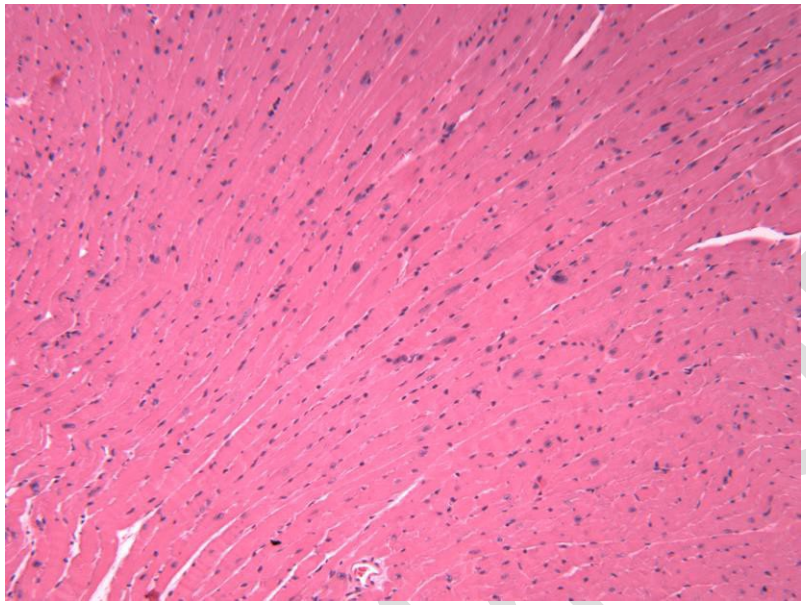

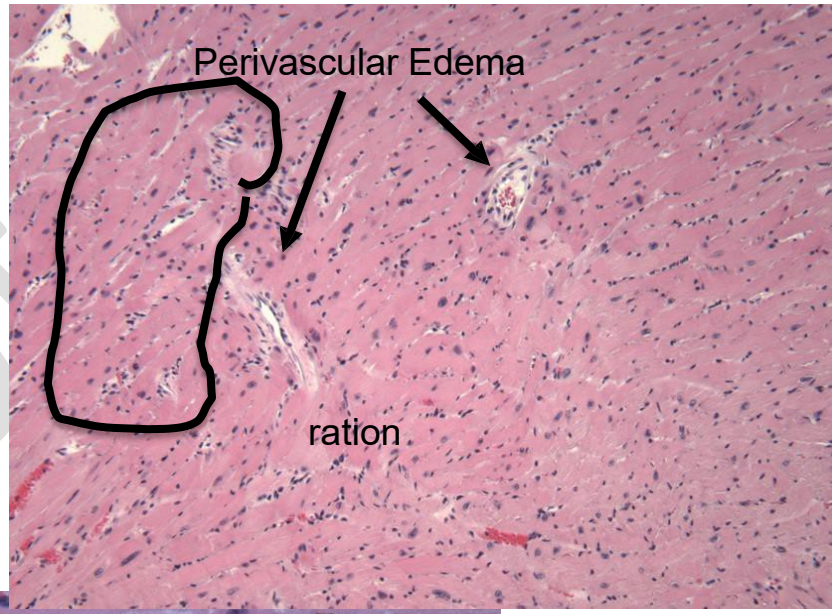

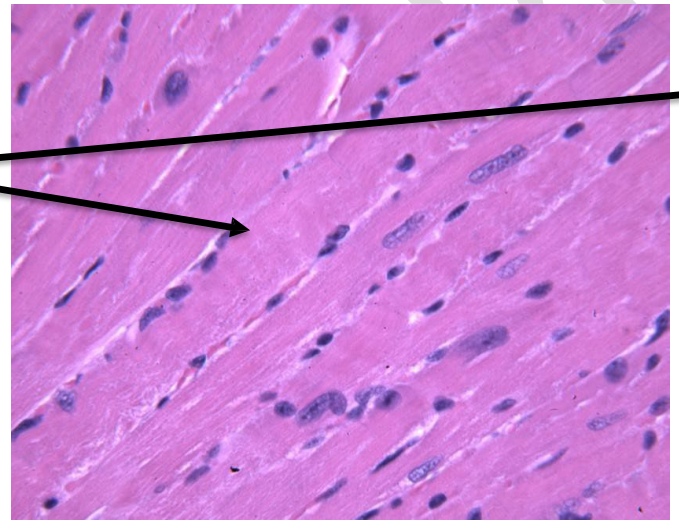

Myofibril Derangement
(fibrils with bands vs not)

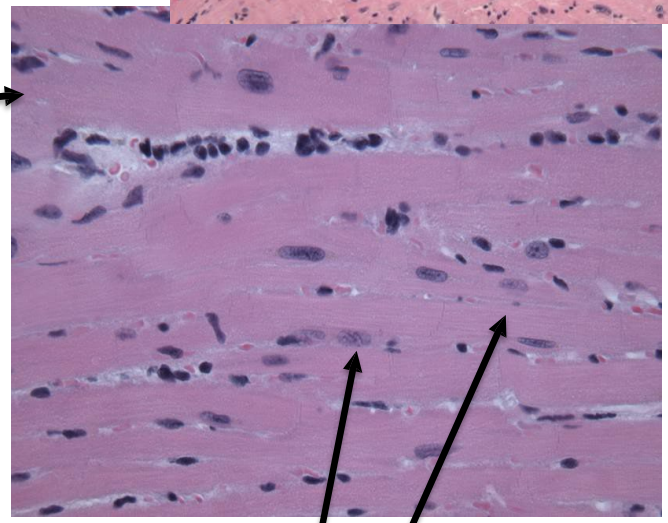

Nuclear Hydrops (swollen, “ghost” nuclei)

Scores
0 = no injury
1 = minimal (0-25%of the section)
2 = mild (25-50%)
3 = significant (50-75%)
4 = severe (more than 75%)

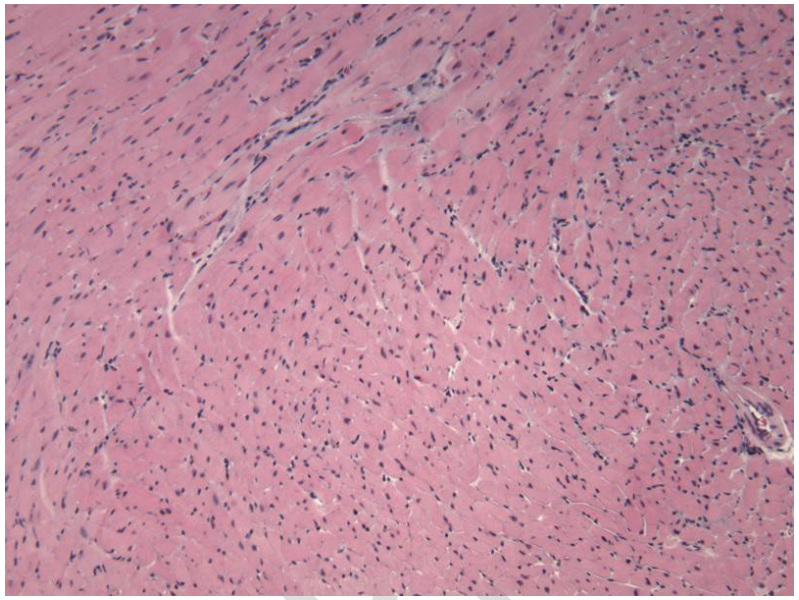

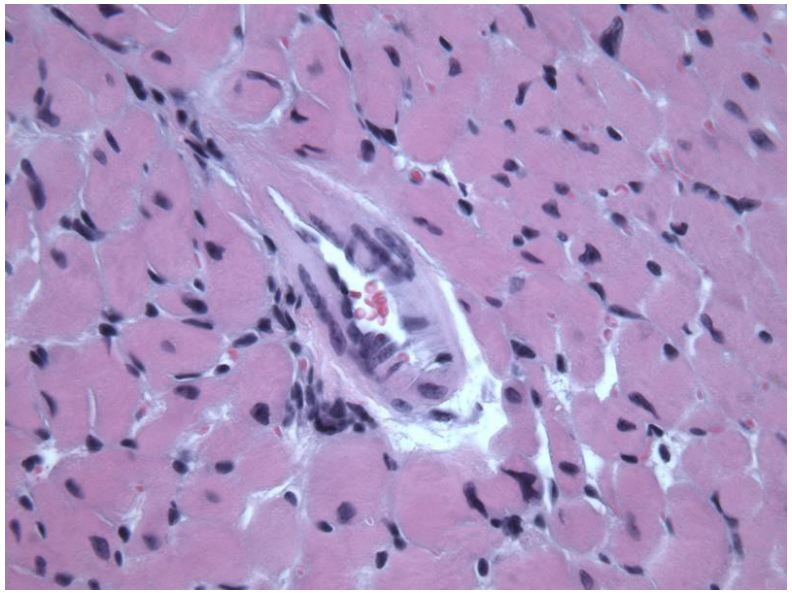

	10x	40x
Perivascular Edema (10X)	2	
Myofibril Derangement (40X)		3
Infiltration of Neutrophils (10X)	3	

Nuclear Hydrops (40X)	1

Total

Scores
0 = no injury
1 = minimal (0-25%of the section)
2 = mild (25-50%)
3 = significant (50-75%)
4 = severe (more than 75%)

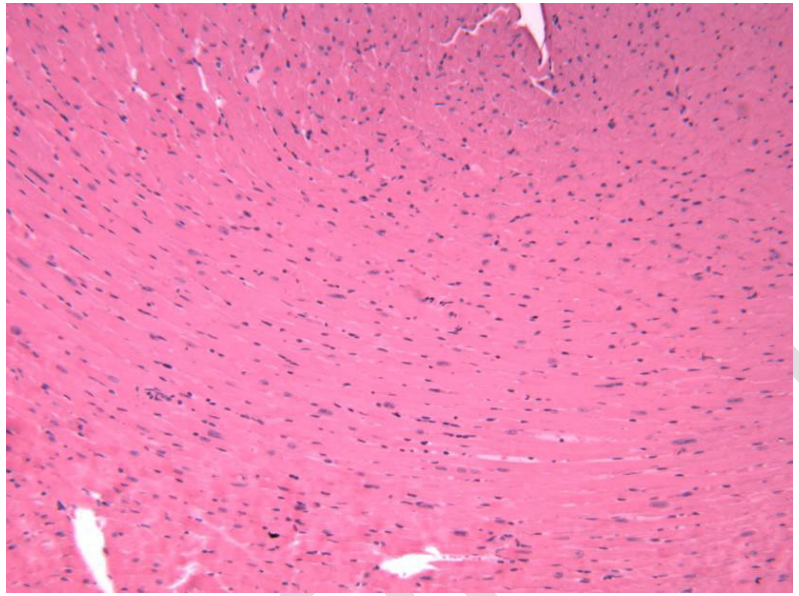

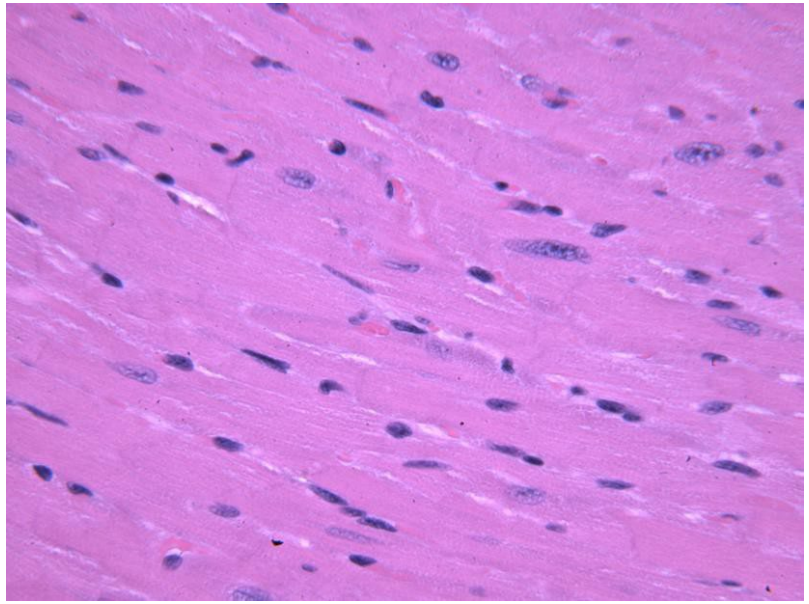

	10x	40x
Perivascular Edema (10X)	0	
Myofibril Derangement (40X)		1
Infiltration of Neutrophils (10X)	1	
Nuclear Hydrops (40X)		0

Scores
0 = no injury
1 = minimal (0-25%of the section)
2 = mild (25-50%)
3 = significant (50-75%)
4 = severe (more than 75%)

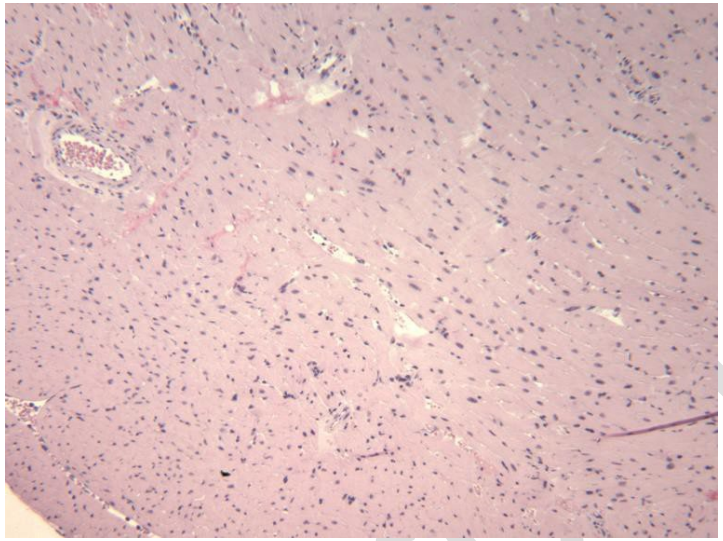

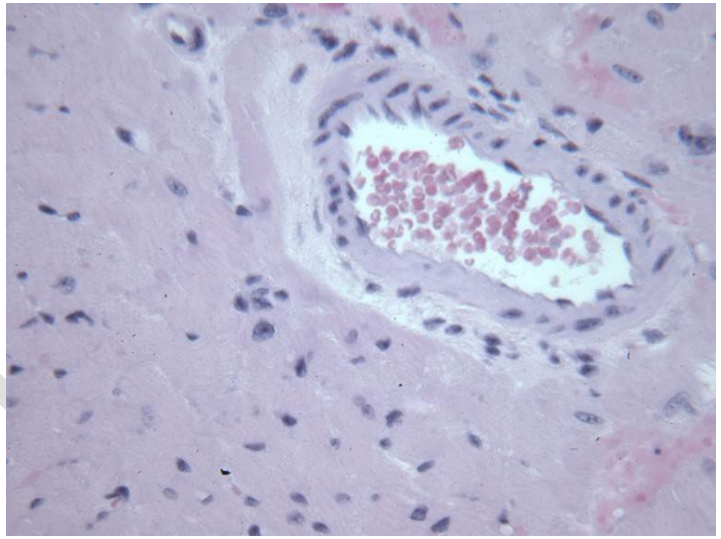

	10x	40x
Perivascular Edema (10X)	3	
Myofibril Derangement (40X)		3
Infiltration of Neutrophils (10X)	3	
Nuclear Hydrops (40X)		3
Total		

Scores

Scores

0 = no injury
1 = minimal (0-25%of the section)
2 = mild (25-50%)
3 = significant (50-75%)
4 = severe (more than 75%)

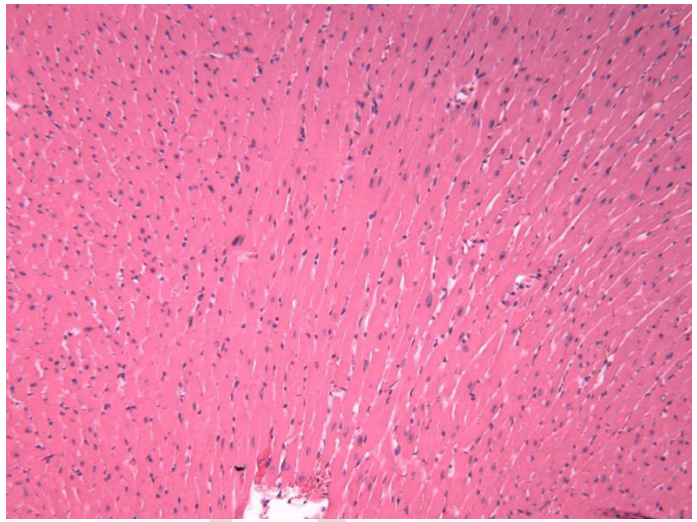

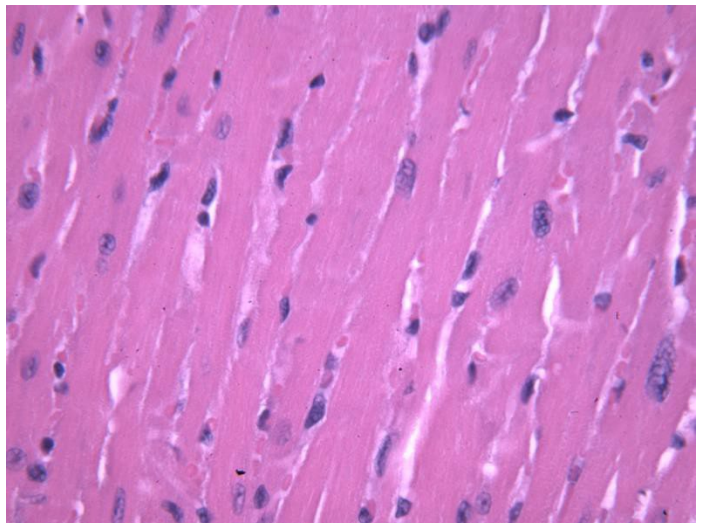

	10x	40x
Perivascular Edema (10X)	1	
Myofibril Derangement (40X)		1
Infiltration of Neutrophils (10X)	2	
Nuclear Hydrops (40X)		0
Total		